

# Analysis of a pseudostress-based mixed finite element method for the Brinkman model of porous media flow\*

GABRIEL N. GATICA<sup>†</sup> LUIS F. GATICA<sup>‡</sup> ANTONIO MÁRQUEZ<sup>§</sup>

## Abstract

In this paper we introduce and analyze a new mixed finite element method for the Brinkman model of porous media flow with mixed boundary conditions. We use a dual-mixed formulation in which the main unknown is given by the pseudostress. The original velocity and pressure unknowns are easily recovered through a simple postprocessing. In addition, since the Neumann boundary condition becomes essential, we impose it in a weak sense, which yields the introduction of the trace of the fluid velocity over the Neumann boundary as the associated Lagrange multiplier. We apply the Babuska-Brezzi theory to establish sufficient conditions for the well-posedness of the resulting continuous and discrete formulations. In particular, a feasible choice of finite element subspaces is given by Raviart-Thomas elements of order  $k \geq 0$  for the pseudostress, and continuous piecewise polynomials of degree  $k + 1$  for the Lagrange multiplier. We also derive a reliable and efficient residual-based a posteriori error estimator for this problem. Suitable auxiliary problems, the continuous inf-sup conditions satisfied by the bilinear forms involved, a discrete Helmholtz decomposition, and the local approximation properties of the Raviart-Thomas and Clément interpolation operators are the main tools for proving the reliability. Then, Helmholtz's decomposition, inverse inequalities, and the localization technique based on triangle-bubble and edge-bubble functions are employed to show the efficiency. Finally, several numerical results illustrating the performance of the method, confirming the theoretical properties of the estimator, and showing the behaviour of the associated adaptive algorithm, are provided.

**Key words:** Brinkman model, mixed finite elements, pseudostress

**Mathematics subject classifications (1991):** 65N30, 65N12, 65N15, 65J15, 74B20

## 1 Introduction

The derivation of pseudostress-based mixed finite element methods for linear and nonlinear problems in continuum mechanics has become a very active research area during recent years. This fact has been strongly motivated by the need of finding new ways of circumventing the main drawback of the usual stress-based approach, namely the symmetry requirement of this tensor. While the weak imposition of this condition through the introduction of a suitable Lagrange multiplier (rotation in elasticity and

---

\*This research was partially supported by BASAL project CMM, Universidad de Chile, by Centro de Investigación en Ingeniería Matemática (CI<sup>2</sup>MA), Universidad de Concepción, by CONICYT-Chile through the Fondecyt project 1080392, and by Dirección de Investigación, Universidad Católica de la Santísima Concepción.

<sup>†</sup>CI<sup>2</sup>MA - Universidad de Concepción, and Departamento de Ingeniería Matemática, Facultad de Ciencias Físicas y Matemáticas, Universidad de Concepción, Casilla 160-C, Concepción, Chile, email: [ggatica@ing-mat.udec.cl](mailto:ggatica@ing-mat.udec.cl)

<sup>‡</sup>CI<sup>2</sup>MA - Universidad de Concepción, and Facultad de Ingeniería, Universidad Católica de la Santísima Concepción, Casilla 297, Concepción, Chile, email: [lgatica@ucsc.cl](mailto:lgatica@ucsc.cl)

<sup>§</sup>Departamento de Construcción e Ingeniería de Fabricación, Universidad de Oviedo, Oviedo, España, email: [amarquez@uniovi.es](mailto:amarquez@uniovi.es)

vorticity in fluid mechanics) was suggested long before (see, e.g. [3]), the use of the pseudostress has become very popular lately, specially in the context of least-squares and augmented methods for incompressible flows, mainly because of the non-necessity of the symmetry condition. This fact yielded the appearing of two new approaches: the velocity-pressure-pseudostress and velocity-pseudostress formulations (see, e.g. [9], [10], [19], and the references therein). In particular, augmented mixed finite element methods for both pseudostress-based formulations of the stationary Stokes equations, which extends analogue results for linear elasticity problems (see [21] and [24]), are introduced and analyzed in [19]. In addition, the corresponding augmented mixed finite element schemes for the velocity-pressure-stress formulation of the Stokes problem, in which the vorticity is introduced as the Lagrange multiplier taking care of the weak symmetry of the stress, are studied in [18]. On the other hand, the velocity-pressure-pseudostress formulation has also been applied to nonlinear Stokes problems (see, e.g. [17], [22], [31]), which includes models arising in quasi-Newtonian fluids, extensions to the setting of reflexive Banach spaces (with applications to nonlinear models such as the Carreau law for viscoplastic flows), the use of trace-free tensors for the velocity gradient, and the incorporation of three-field formulations with the pseudostress, the velocity, and the velocity gradient as unknowns.

However, in spite of the above mentioned works, it is surprising to realize that mixed finite element methods for the pure velocity-pseudostress formulation of the Stokes equations, that is without augmenting or employing least-squares terms, had not been studied until [11]. It is shown there that Raviart-Thomas elements of index  $k \geq 0$  for the pseudostress and piecewise discontinuous polynomials of degree  $k$  for the velocity lead to a stable Galerkin scheme with quasi-optimal accuracy. The pressure and all the other physical quantities of interest can be computed in a postprocessing procedure without affecting the accuracy of approximation. The formulation from [11] is modified in [25] by incorporating the pressure unknown into the discrete analysis, thus allowing further flexibility for approximating this unknown. More precisely, it is established there that the corresponding Galerkin scheme only makes sense for pressure finite element subspaces not containing the traces of the pseudostresses subspace. In particular, this is the case when Raviart-Thomas elements of index  $k \geq 0$  for the pseudostress, and piecewise discontinuous polynomials of degree  $k$  for the velocity and the pressure, are utilized. Otherwise, both discrete schemes coincide and hence one obviously stays with the simplest one. Furthermore, reliable and efficient residual-based a posteriori error estimators for both Galerkin schemes (without and with pressure) are also derived in [25]. More recently, the analysis from [11] and [25] is extended in [26] to the class of nonlinear problems originally studied in [22] and [31]. Indeed, the results in [26] refer to the a priori and a posteriori error analyses of the velocity-pseudostress approach as applied to quasi-Newtonian Stokes flows whose kinematic viscosities are a nonlinear monotone function of the velocity gradient of the fluid. The latter is introduced as an auxiliary unknown, and the pressure is eliminated using the incompressibility condition, whence the resulting variational formulation shows a twofold saddle point structure (as in [22] and [31]). An augmented version of this formulation, which simplifies the requirements for well-posedness of the associated Galerkin scheme, is also introduced and analyzed there.

On the other hand, a quite interesting problem in fluid mechanics for which, up to the authors' knowledge, no stress-based or pseudostress-based approaches seem to be available, is the Brinkman model of porous media flow. Actually, all the formulations found in the literature are based on the typical Stokes-type (also called primal-mixed) formulation in which the velocity and the pressure are kept as the main unknowns. The corresponding equations, which can be seen as a mixture of Darcy's and Stokes' equations, are hard to solve, firstly because of the wide range of possible permeability ratios, and secondly due to the nature of the mixed boundary conditions involved. One way of solving the first issue is by means of stabilized methods (see, e.g. [8], [32]), whereas the weak imposition of the Dirichlet boundary conditions, using Nitsche's method, has been applied recently to deal with

the second difficulty (see, e.g. [29] and the references therein). According to the above, and in order to provide an alternative way of dealing with the mixed boundary conditions, as well as to further contribute in the numerical analysis of this problem, in the present work we develop the a priori and a posteriori error analyses of a dual-mixed approach in which the pseudostress  $\boldsymbol{\sigma}$  is the main unknown of the resulting saddle point problem, and the velocity and pressure are easily recovered in terms of  $\boldsymbol{\sigma}$  through simple postprocessing formulae. In addition, as it is usual for dual-mixed methods, the Dirichlet boundary condition for the velocity becomes natural in this case, and the Neumann boundary condition, being essential, is imposed weakly through the introduction of the trace of the velocity on that boundary as the associated Lagrange multiplier. The rest of the paper is organized as follows. In Section 2 we define the Brinkman model, derive the pseudostress-based dual-mixed formulation, and then show that it is well-posed. The associated mixed finite element method is introduced and analyzed in Section 3. Next, in Section 4 we derive a reliable and efficient residual-based a posteriori error estimator. Finally, some numerical results showing the good performance of the mixed finite element methods, confirming the reliability and efficiency of the estimator, and illustrating the behaviour of the associated adaptive algorithm are reported in Section 5.

We end this section with some notations to be used below. Given  $\boldsymbol{\tau} := (\tau_{ij})$ ,  $\boldsymbol{\zeta} := (\zeta_{ij}) \in \mathbb{R}^{2 \times 2}$ , we write as usual

$$\boldsymbol{\tau}^t := (\tau_{ji}), \quad \text{tr}(\boldsymbol{\tau}) := \sum_{i=1}^2 \tau_{ii}, \quad \boldsymbol{\tau}^d := \boldsymbol{\tau} - \frac{1}{2} \text{tr}(\boldsymbol{\tau}) \mathbf{I}, \quad \text{and} \quad \boldsymbol{\tau} : \boldsymbol{\zeta} := \sum_{i,j=1}^2 \tau_{ij} \zeta_{ij},$$

where  $\mathbf{I}$  is the identity matrix of  $\mathbb{R}^{2 \times 2}$ . In addition, in what follows we utilize standard simplified terminology for Sobolev spaces and norms. In particular, if  $\mathcal{O}$  is a domain,  $\mathcal{S}$  is a Lipschitz curve, and  $r \in \mathbb{R}$ , we define

$$\mathbf{H}^r(\mathcal{O}) := [H^r(\mathcal{O})]^2, \quad \mathbb{H}^r(\mathcal{O}) := [H^r(\mathcal{O})]^{2 \times 2}, \quad \text{and} \quad \mathbf{H}^r(\mathcal{S}) := [H^r(\mathcal{S})]^2.$$

However, when  $r = 0$  we usually write  $\mathbf{L}^2(\mathcal{O})$ ,  $\mathbb{L}^2(\mathcal{O})$ , and  $\mathbf{L}^2(\mathcal{S})$  instead of  $\mathbf{H}^0(\mathcal{O})$ ,  $\mathbb{H}^0(\mathcal{O})$ , and  $\mathbf{H}^0(\mathcal{S})$ , respectively. The corresponding norms are denoted by  $\|\cdot\|_{r,\mathcal{O}}$  (for  $H^r(\mathcal{O})$ ,  $\mathbf{H}^r(\mathcal{O})$ , and  $\mathbb{H}^r(\mathcal{O})$ ) and  $\|\cdot\|_{r,\mathcal{S}}$  (for  $H^r(\mathcal{S})$  and  $\mathbf{H}^r(\mathcal{S})$ ). In general, given any Hilbert space  $H$ , we use  $\mathbf{H}$  and  $\mathbb{H}$  to denote  $H^2$  and  $H^{2 \times 2}$ , respectively. In turn, the Hilbert space

$$\mathbf{H}(\text{div}; \mathcal{O}) := \{\mathbf{w} \in \mathbf{L}^2(\mathcal{O}) : \text{div } \mathbf{w} \in L^2(\mathcal{O})\},$$

is standard in the realm of mixed problems (see [7]). The space of matrix valued functions whose rows belong to  $\mathbf{H}(\text{div}; \mathcal{O})$  will be denoted  $\mathbb{H}(\mathbf{div}; \mathcal{O})$ . The Hilbert norms of  $\mathbf{H}(\text{div}; \mathcal{O})$  and  $\mathbb{H}(\mathbf{div}; \mathcal{O})$  are denoted by  $\|\cdot\|_{\text{div};\mathcal{O}}$  and  $\|\cdot\|_{\mathbf{div};\mathcal{O}}$ , respectively. Note that if  $\boldsymbol{\tau} \in \mathbb{H}(\mathbf{div}; \mathcal{O})$ , then  $\mathbf{div } \boldsymbol{\tau} \in L^2(\mathcal{O})$ . Finally, we employ  $\mathbf{0}$  to denote a generic null vector (including the null functional and operator), and use  $C$  and  $c$ , with or without subscripts, bars, tildes or hats, to denote generic constants independent of the discretization parameters, which may take different values at different places.

## 2 The Brinkman model and the pseudostress-based formulation

### 2.1 The boundary value problem

Let  $\Omega$  be a bounded and simply connected domain in  $\mathbb{R}^2$  with polygonal boundary  $\Gamma$ , and such that all its interior angles lie in  $(0, 2\pi)$ . Also, let  $\Gamma_D$  and  $\Gamma_N$  be disjoint open subsets of  $\Gamma$ , with  $|\Gamma_D|$ ,  $|\Gamma_N| \neq 0$ , such that  $\Gamma = \bar{\Gamma}_D \cup \bar{\Gamma}_N$ . Then, given  $\mathbf{f} \in \mathbf{L}^2(\Omega)$  and  $\mathbf{g} \in \mathbf{H}^{-1/2}(\Gamma_N)$ , our boundary value

problem reads as follows: Find a tensor field  $\boldsymbol{\sigma}$  (pseudostress), a vector field  $\mathbf{u}$  (velocity), and a scalar field  $p$  (pressure) in appropriate spaces such that

$$\begin{aligned} \boldsymbol{\sigma} &= \mu \nabla \mathbf{u} - p \mathbf{I} \quad \text{in } \Omega, & \alpha \mathbf{u} - \mathbf{div}(\boldsymbol{\sigma}) &= \mathbf{f} \quad \text{in } \Omega, & \mathbf{div}(\mathbf{u}) &= 0 \quad \text{in } \Omega, \\ \mathbf{u} &= \mathbf{0} \quad \text{on } \Gamma_D, & \boldsymbol{\sigma} \boldsymbol{\nu} &= \mathbf{g} \quad \text{on } \Gamma_N, \end{aligned} \quad (2.1)$$

where  $\mu$  is the effective viscosity,  $\alpha$  is the viscosity divided by the permeability,  $\boldsymbol{\nu}$  is the unit outward normal to  $\Gamma$ , and  $\mathbf{div}$  denotes the usual divergence operator  $\mathbf{div}$  acting along each row of the corresponding tensor. We recall here that the Sobolev space  $\mathbf{H}^{-1/2}(\Gamma_N)$  is defined as the dual of  $\mathbf{H}_{00}^{1/2}(\Gamma_N)$ , where

$$\mathbf{H}_{00}^{1/2}(\Gamma_N) := \left\{ \mathbf{v}|_{\Gamma_N} : \mathbf{v} \in \mathbf{H}^1(\Omega), \mathbf{v} = \mathbf{0} \quad \text{on } \Gamma_D \right\}.$$

The corresponding duality pairing with respect to the  $\mathbf{L}^2(\Gamma_N)$  - inner product is denoted by  $\langle \cdot, \cdot \rangle_{\Gamma_N}$ . In addition, throughout the paper  $\| \cdot \|_{0;1/2,\Gamma_N}$  stands for the usual norms of  $H_{00}^{1/2}(\Gamma_N)$  and  $\mathbf{H}_{00}^{1/2}(\Gamma_N)$ .

Now, we note that the pair of equations given by

$$\boldsymbol{\sigma} = \mu \nabla \mathbf{u} - p \mathbf{I} \quad \text{in } \Omega, \quad \text{and} \quad \mathbf{div}(\mathbf{u}) = 0 \quad \text{in } \Omega,$$

is equivalent to

$$\boldsymbol{\sigma} = \mu \nabla \mathbf{u} - p \mathbf{I} \quad \text{in } \Omega, \quad \text{and} \quad p = -\frac{1}{2} \text{tr}(\boldsymbol{\sigma}) \quad \text{in } \Omega, \quad (2.2)$$

whence (2.1) can be rewritten as

$$\begin{aligned} \frac{1}{\mu} \boldsymbol{\sigma}^d &= \nabla \mathbf{u} \quad \text{in } \Omega, & \alpha \mathbf{u} - \mathbf{div}(\boldsymbol{\sigma}) &= \mathbf{f} \quad \text{in } \Omega, \\ \mathbf{u} &= \mathbf{0} \quad \text{on } \Gamma_D, & \boldsymbol{\sigma} \boldsymbol{\nu} &= \mathbf{g} \quad \text{on } \Gamma_N. \end{aligned} \quad (2.3)$$

## 2.2 The dual-mixed formulation

Initially we test the first equation of (2.3) with  $\boldsymbol{\tau} \in \mathbb{H}(\mathbf{div}; \Omega)$  and use that  $\text{tr}(\boldsymbol{\tau}^d) = 0$ . Then, integrating by parts the expression  $\int_{\Omega} \nabla \mathbf{u} : \boldsymbol{\tau}$ , using the Dirichlet boundary condition, and introducing the auxiliary unknown  $\boldsymbol{\xi} := -\mathbf{u}|_{\Gamma_N} \in \mathbf{H}_{00}^{1/2}(\Gamma_N)$ , we arrive at

$$\frac{1}{\mu} \int_{\Omega} \boldsymbol{\sigma}^d : \boldsymbol{\tau}^d + \int_{\Omega} \mathbf{u} \cdot \mathbf{div}(\boldsymbol{\tau}) + \langle \boldsymbol{\tau} \boldsymbol{\nu}, \boldsymbol{\xi} \rangle_{\Gamma_N} = 0 \quad \forall \boldsymbol{\tau} \in \mathbb{H}(\mathbf{div}; \Omega). \quad (2.4)$$

In turn, the Neumann boundary condition is imposed weakly as

$$\langle \boldsymbol{\sigma} \boldsymbol{\nu}, \boldsymbol{\lambda} \rangle_{\Gamma_N} = \langle \mathbf{g}, \boldsymbol{\lambda} \rangle_{\Gamma_N} \quad \forall \boldsymbol{\lambda} \in \mathbf{H}_{00}^{1/2}(\Gamma_N).$$

Finally, replacing  $\mathbf{u}$  in (2.4) by

$$\mathbf{u} = \frac{1}{\alpha} \left\{ \mathbf{f} + \mathbf{div}(\boldsymbol{\sigma}) \right\} \quad \text{in } \Omega, \quad (2.5)$$

we obtain the variational formulation: Find  $(\boldsymbol{\sigma}, \boldsymbol{\xi}) \in \mathbb{H}(\mathbf{div}; \Omega) \times \mathbf{H}_{00}^{1/2}(\Gamma_N)$  such that

$$\begin{aligned} \frac{1}{\mu} \int_{\Omega} \boldsymbol{\sigma}^d : \boldsymbol{\tau}^d + \frac{1}{\alpha} \int_{\Omega} \mathbf{div}(\boldsymbol{\sigma}) \cdot \mathbf{div}(\boldsymbol{\tau}) + \langle \boldsymbol{\tau} \boldsymbol{\nu}, \boldsymbol{\xi} \rangle_{\Gamma_N} &= -\frac{1}{\alpha} \int_{\Omega} \mathbf{f} \cdot \mathbf{div}(\boldsymbol{\tau}), \\ \langle \boldsymbol{\sigma} \boldsymbol{\nu}, \boldsymbol{\lambda} \rangle_{\Gamma_N} &= \langle \mathbf{g}, \boldsymbol{\lambda} \rangle_{\Gamma_N}. \end{aligned} \quad (2.6)$$

for all  $(\boldsymbol{\tau}, \boldsymbol{\lambda}) \in \mathbb{H}(\mathbf{div}; \Omega) \times \mathbf{H}_{00}^{1/2}(\Gamma_N)$ .

Equivalently, (2.6) can be rewritten as the following saddle point problem: Find  $(\boldsymbol{\sigma}, \boldsymbol{\xi}) \in H \times Q$  such that

$$\begin{aligned} a(\boldsymbol{\sigma}, \boldsymbol{\tau}) + b(\boldsymbol{\tau}, \boldsymbol{\xi}) &= -\frac{1}{\alpha} \int_{\Omega} \mathbf{f} \cdot \mathbf{div}(\boldsymbol{\tau}) \quad \forall \boldsymbol{\tau} \in H, \\ b(\boldsymbol{\sigma}, \boldsymbol{\lambda}) &= \langle \mathbf{g}, \boldsymbol{\lambda} \rangle_{\Gamma_N} \quad \forall \boldsymbol{\lambda} \in Q, \end{aligned} \quad (2.7)$$

where  $H := \mathbb{H}(\mathbf{div}; \Omega)$ ,  $Q := \mathbf{H}_{00}^{1/2}(\Gamma_N)$ , and  $a : H \times H \rightarrow \mathbb{R}$  and  $b : H \times Q \rightarrow \mathbb{R}$  are the bounded bilinear forms defined by

$$a(\boldsymbol{\zeta}, \boldsymbol{\tau}) := \frac{1}{\mu} \int_{\Omega} \boldsymbol{\zeta}^{\mathbf{d}} : \boldsymbol{\tau}^{\mathbf{d}} + \frac{1}{\alpha} \int_{\Omega} \mathbf{div}(\boldsymbol{\zeta}) \cdot \mathbf{div}(\boldsymbol{\tau}) \quad \forall \boldsymbol{\zeta}, \boldsymbol{\tau} \in H,$$

and

$$b(\boldsymbol{\tau}, \boldsymbol{\lambda}) := \langle \boldsymbol{\tau}\boldsymbol{\nu}, \boldsymbol{\lambda} \rangle_{\Gamma_N} \quad \forall \boldsymbol{\tau} \in H, \quad \forall \boldsymbol{\lambda} \in Q.$$

Note that the bounded linear operator  $\mathbf{B} : H \rightarrow Q$  induced by the bilinear form  $b$  is given by

$$\mathbf{B}(\boldsymbol{\tau}) := \mathcal{R}_0(\boldsymbol{\tau}\boldsymbol{\nu}) \quad \forall \boldsymbol{\tau} \in H,$$

where  $\mathcal{R}_0 : \mathbf{H}^{-1/2}(\Gamma_N) \rightarrow \mathbf{H}_{00}^{1/2}(\Gamma_N)$  is the corresponding Riesz operator.

### 2.3 Analysis of the dual-mixed formulation

In what follows we show the well-posedness of (2.7). We begin the analysis with the inf-sup condition for the bilinear form  $b$ , which is equivalent to the surjectivity of  $\mathbf{B}$ .

**Lemma 2.1** *There exists a positive constant  $\beta$ , depending only on  $\Omega$ , such that*

$$\sup_{\substack{\boldsymbol{\tau} \in H \\ \boldsymbol{\tau} \neq \mathbf{0}}} \frac{b(\boldsymbol{\tau}, \boldsymbol{\lambda})}{\|\boldsymbol{\tau}\|_{\mathbf{div}; \Omega}} \geq \beta \|\boldsymbol{\lambda}\|_{0; 1/2, \Gamma_N} \quad \forall \boldsymbol{\lambda} \in Q.$$

**Proof.** Given  $\boldsymbol{\lambda} \in \mathbf{H}_{00}^{1/2}(\Gamma_N)$ ,  $\boldsymbol{\lambda} \neq \mathbf{0}$ , we let  $\mathbf{z} \in \mathbf{H}^1(\Omega)$  be the unique weak solution of the problem

$$-\Delta \mathbf{z} = \mathbf{0} \quad \text{in } \Omega, \quad \mathbf{z} = \mathbf{0} \quad \text{on } \Gamma_D, \quad \nabla \mathbf{z}\boldsymbol{\nu} = \mathcal{R}_0^{-1}(\boldsymbol{\lambda}) \quad \text{on } \Gamma_N,$$

and define  $\widehat{\boldsymbol{\tau}} := \nabla \mathbf{z}$  in  $\Omega$ . It follows that  $\mathbf{div}(\widehat{\boldsymbol{\tau}}) = \mathbf{0}$  in  $\Omega$ , which shows that  $\widehat{\boldsymbol{\tau}} \in \mathbb{H}(\mathbf{div}; \Omega)$ , and then  $\widehat{\boldsymbol{\tau}}\boldsymbol{\nu} = \mathcal{R}_0^{-1}(\boldsymbol{\lambda})$  on  $\Gamma_N$ . Hence, it is clear that  $\mathbf{B}(\widehat{\boldsymbol{\tau}}) = \boldsymbol{\lambda}$ , which proves that  $\mathbf{B}$  is surjective.  $\square$

Next, we let  $\mathbf{V}$  be the kernel of  $\mathbf{B}$ , that is  $\mathbf{V} := \left\{ \boldsymbol{\tau} \in H : \boldsymbol{\tau}\boldsymbol{\nu} = \mathbf{0} \quad \text{on } \Gamma_N \right\}$ , and prove that the bilinear form  $a$  is  $\mathbf{V}$ -elliptic. To this end, we first consider the decomposition

$$\mathbb{H}(\mathbf{div}; \Omega) = \mathbb{H}_0(\mathbf{div}; \Omega) \oplus \mathbb{R} \mathbf{I},$$

where  $\mathbb{H}_0(\mathbf{div}; \Omega) := \left\{ \boldsymbol{\tau} \in \mathbb{H}(\mathbf{div}; \Omega) : \int_{\Omega} \text{tr}(\boldsymbol{\tau}) = 0 \right\}$ . This means that for any  $\boldsymbol{\tau} \in \mathbb{H}(\mathbf{div}; \Omega)$  there exist unique  $\boldsymbol{\tau}_0 \in \mathbb{H}_0(\mathbf{div}; \Omega)$  and  $d := \frac{1}{|\Omega|} \int_{\Omega} \text{tr}(\boldsymbol{\tau}) \in \mathbb{R}$  such that  $\boldsymbol{\tau} = \boldsymbol{\tau}_0 + d\mathbf{I}$ , whence  $\|\boldsymbol{\tau}\|_{\mathbf{div}; \Omega}^2 = \|\boldsymbol{\tau}_0\|_{\mathbf{div}; \Omega}^2 + 2d^2|\Omega|$ . In addition, we have the following lemmas.

**Lemma 2.2** *There exists  $C_1 > 0$ , depending only on  $\Omega$ , such that*

$$C_1 \|\boldsymbol{\tau}_0\|_{0, \Omega}^2 \leq \|\boldsymbol{\tau}^{\mathbf{d}}\|_{0, \Omega}^2 + \|\mathbf{div}(\boldsymbol{\tau})\|_{0, \Omega}^2 \quad \forall \boldsymbol{\tau} \in \mathbb{H}(\mathbf{div}; \Omega).$$

**Proof.** See [4, Lemma 3.1] or [7, Proposition 3.1, Chapter IV]. □

**Lemma 2.3** *There exists  $C_2 > 0$ , depending only on  $\Gamma_N$  and  $\Omega$ , such that*

$$C_2 \|\boldsymbol{\tau}\|_{\mathbf{div};\Omega}^2 \leq \|\boldsymbol{\tau}_0\|_{\mathbf{div};\Omega}^2 \quad \forall \boldsymbol{\tau} \in \mathbf{V}.$$

**Proof.** See [21, Lemma 2.2]. □

Then the  $\mathbf{V}$ -ellipticity of  $a$  is proved as follows.

**Lemma 2.4** *There exists  $C > 0$ , depending only on  $\Gamma_N$  and  $\Omega$ , such that*

$$a(\boldsymbol{\tau}, \boldsymbol{\tau}) \geq C \|\boldsymbol{\tau}\|_{\mathbf{div};\Omega}^2 \quad \forall \boldsymbol{\tau} \in \mathbf{V}.$$

**Proof.** Applying Lemmas 2.2 and 2.3, we deduce that for each  $\boldsymbol{\tau} \in \mathbf{V}$  there holds

$$\begin{aligned} a(\boldsymbol{\tau}, \boldsymbol{\tau}) &= \frac{1}{\mu} \|\boldsymbol{\tau}^{\mathbf{d}}\|_{0,\Omega}^2 + \frac{1}{\alpha} \|\mathbf{div}(\boldsymbol{\tau})\|_{0,\Omega}^2, \\ &\geq \gamma_1 C_1 \|\boldsymbol{\tau}_0\|_{0,\Omega}^2 + \frac{1}{2\alpha} \|\mathbf{div}(\boldsymbol{\tau}_0)\|_{0,\Omega}^2, \\ &\geq \gamma_2 \|\boldsymbol{\tau}_0\|_{\mathbf{div};\Omega}^2 \geq C \|\boldsymbol{\tau}\|_{\mathbf{div};\Omega}^2, \end{aligned}$$

where  $\gamma_1 := \min\{\frac{1}{\mu}, \frac{1}{2\alpha}\}$ ,  $\gamma_2 := \min\{\gamma_1 C_1, \frac{1}{2\alpha}\}$ , and  $C := C_2 \gamma_2$ . □

The well-posedness of our variational formulation (2.7) is provided by the following theorem.

**Theorem 2.1** *Assume that  $\mathbf{f} \in \mathbf{L}^2(\Omega)$  and  $\mathbf{g} \in \mathbf{H}^{-1/2}(\Gamma_N)$ . Then, there exists a unique solution  $(\boldsymbol{\sigma}, \boldsymbol{\xi}) \in H \times Q$  to (2.7). In addition, there exists a positive constant  $C$ , depending only on  $\Omega$ , such that*

$$\|\boldsymbol{\sigma}\|_{\mathbf{div};\Omega} + \|\boldsymbol{\xi}\|_{0;1/2,\Gamma_N} \leq C \left\{ \|\mathbf{f}\|_{0,\Omega} + \|\mathbf{g}\|_{-1/2,\Gamma_N} \right\}.$$

**Proof.** It suffices to notice, according to Lemmas 2.1 and 2.4, that the bilinear forms  $a$  and  $b$  satisfy the hypotheses of the Babuška-Brezzi theory. Then, a straightforward application of the classical result given by [7, Theorem 1.1 in Chapter II] completes the proof. □

### 3 The mixed finite element method

In this section, we define explicit finite element subspaces  $H_h$  of  $\mathbb{H}(\mathbf{div}; \Omega)$  and  $Q_h$  of  $\mathbf{H}_{00}^{1/2}(\Gamma_N)$  such that the mixed finite element scheme associated with the continuous formulation (2.7) is well posed and stable. For this purpose, let  $\{\mathcal{T}_h\}_{h>0}$  be a regular family of triangulations of the polygonal region  $\bar{\Omega}$  by triangles  $T$  of diameter  $h_T$ , with mesh size  $h := \max\{h_T : T \in \mathcal{T}_h\}$ , and such that all the points in  $\bar{\Gamma}_D \cap \bar{\Gamma}_N$  become vertices of  $\mathcal{T}_h$  for all  $h > 0$ . Also, given an integer  $k \geq 0$  and a subset  $S$  of  $\mathbb{R}^2$ , we denote by  $P_k(S)$  the space of polynomials defined in  $S$  of total degree at most  $k$  defined on  $S$ . Then, for each integer  $k \geq 0$  and for each  $T \in \mathcal{T}_h$ , we define the local Raviart-Thomas space of order  $k$  (see, e.g. [7], [33])

$$RT_k(T) := \mathbf{P}_k(T) \oplus P_k(T) \mathbf{x}$$

where  $\mathbf{x} := \begin{pmatrix} x_1 \\ x_2 \end{pmatrix}$  is a generic vector of  $\mathbb{R}^2$ . The corresponding finite element subspace  $H_h$  for the unknown  $\boldsymbol{\sigma} \in \mathbb{H}(\mathbf{div}; \Omega)$  is given by the global Raviart-Thomas space of order  $k$ , that is,

$$H_h := \left\{ \boldsymbol{\tau} \in \mathbb{H}(\mathbf{div}; \Omega) : (\tau_{i1}, \tau_{i2})^\top \in RT_k(T) \quad \forall i \in \{1, 2\}, \quad \forall T \in \mathcal{T}_h \right\}. \quad (3.1)$$

In turn, an eventual finite element subspace for the fluid velocity  $\mathbf{u}$  would be given by the global space of piecewise polynomials of degree  $\leq k$ , that is

$$\mathcal{Q}_h^{\mathbf{u}} := \left\{ \mathbf{v} \in \mathbf{L}^2(\Omega) : \mathbf{v}|_T \in \mathbf{P}_k(T) \quad \forall T \in \mathcal{T}_h \right\}. \quad (3.2)$$

Next, let  $\Sigma_h$  be the partition on  $\Gamma_N$  induced by the triangulation  $\mathcal{T}_h$ , and define the mesh size  $h_\Sigma := \max \{|e| : e \in \Sigma_h\}$ . Then we consider two possible choices for  $Q_h$ , the finite element subspace for the unknown  $\boldsymbol{\xi} \in \mathbf{H}_{00}^{1/2}(\Gamma_N)$ .

**A first choice for  $Q_h$ :** Let  $\Sigma_{\tilde{h}}$  be another partition of  $\Gamma_N$ , completely independent from  $\Sigma_h$ , with  $\tilde{h} := \max \{|e| : e \in \Sigma_{\tilde{h}}\}$ . Then, given an integer  $k \geq 0$ , we define

$$Q_h := \left\{ \boldsymbol{\lambda}_{\tilde{h}} \in \mathbf{H}_{00}^{1/2}(\Gamma_N) : \boldsymbol{\lambda}_{\tilde{h}}|_e \in \mathbf{P}_{k+1}(e) \quad \forall e \in \Sigma_{\tilde{h}} \right\}. \quad (3.3)$$

**A second choice for  $Q_h$ :** Let us assume that the number of edges of  $\Sigma_h$  is an even number. Then, we let  $\Sigma_{2h}$  be the partition of  $\Gamma_N$  arising by joining pairs of adjacent elements, and define for  $k = 0$

$$Q_h := \left\{ \boldsymbol{\lambda}_h \in \mathbf{H}_{00}^{1/2}(\Gamma_N) : \boldsymbol{\lambda}_h|_e \in \mathbf{P}_1(e) \quad \forall e \in \Sigma_{2h} \right\}. \quad (3.4)$$

Then, the mixed finite element scheme associated with (2.7) reads : Find  $(\boldsymbol{\sigma}_h, \boldsymbol{\xi}_h) \in H_h \times Q_h$  such that

$$\begin{aligned} a(\boldsymbol{\sigma}_h, \boldsymbol{\tau}_h) + b(\boldsymbol{\tau}_h, \boldsymbol{\xi}_h) &= -\frac{1}{\alpha} \int_{\Omega} \mathbf{f} \cdot \mathbf{div}(\boldsymbol{\tau}_h) \quad \forall \boldsymbol{\tau}_h \in H_h, \\ b(\boldsymbol{\sigma}_h, \boldsymbol{\lambda}_h) &= \langle \mathbf{g}, \boldsymbol{\lambda}_h \rangle_{\Gamma_N} \quad \forall \boldsymbol{\lambda}_h \in Q_h. \end{aligned} \quad (3.5)$$

It is important to remark at this point that the second identity in (2.2) certainly suggests that the pressure  $p$  can be approximated later on by the postprocessing formula

$$p_h := -\frac{1}{2} \operatorname{tr}(\boldsymbol{\sigma}_h). \quad (3.6)$$

In what follows we apply the discrete Babuška-Brezzi theory to show that (3.5) is well posed. We begin with the proof of the discrete inf-sup condition for  $b$ , which establishes the existence of  $\beta > 0$ , independent of  $h$ , such that

$$\sup_{\substack{\boldsymbol{\tau}_h \in H_h \\ \boldsymbol{\tau}_h \neq \mathbf{0}}} \frac{\langle \boldsymbol{\tau}_h \boldsymbol{\nu}, \boldsymbol{\lambda}_h \rangle_{\Gamma_N}}{\|\boldsymbol{\tau}_h\|_{\mathbf{div}; \Omega}} \geq \beta \|\boldsymbol{\lambda}_h\|_{0; 1/2, \Gamma_N} \quad \forall \boldsymbol{\lambda}_h \in Q_h. \quad (3.7)$$

**Lemma 3.1** *Let  $Q_h$  be given by (3.3) and assume that both  $\Sigma_h$  and  $\Sigma_{\tilde{h}}$  are quasi-uniform. Then there exist constants  $C_0 \in (0, 1]$  and  $\beta > 0$ , independent of  $h$  and  $\tilde{h}$ , such that whenever  $h_\Sigma \leq C_0 \tilde{h}$ , there holds (3.7).*

**Proof.** It proceeds similarly to the proofs of [5, Lemmas 3.2 and 3.3]. We omit further details.  $\square$

**Lemma 3.2** *Let  $Q_h$  be given by (3.4) and assume that  $\mathcal{T}_h$  is quasi-uniform in a neighborhood of  $\Gamma_N$ . Then there exists  $\beta > 0$ , independent of  $h$ , such that (3.7) holds.*

**Proof.** It follows as in the proof of [27, Lemma 5.2]. We refer to [27, Section 4.3 and 5] for full details.  $\square$

We now aim to show the  $\mathbf{V}_h$ -ellipticity of the bilinear form  $a$ , where  $\mathbf{V}_h$  is the discrete kernel of the operator induced by  $b$ , that is

$$\mathbf{V}_h := \left\{ \boldsymbol{\tau}_h \in H_h : \langle \boldsymbol{\tau}_h \boldsymbol{\nu}, \boldsymbol{\lambda}_h \rangle_{\Gamma_N} = 0 \quad \forall \boldsymbol{\lambda}_h \in Q_h \right\}.$$

The following result provides the discrete analogue of Lemma 2.3.

**Lemma 3.3** *Assume that there exists a fixed  $\tilde{\boldsymbol{\lambda}} \in \mathbf{H}_{00}^{1/2}(\Gamma_N)$  such that  $\tilde{\boldsymbol{\lambda}} \in Q_h$  for all  $h > 0$  and  $\langle \boldsymbol{\nu}, \tilde{\boldsymbol{\lambda}} \rangle_{\Gamma_N} \neq 0$ . Then there exists  $C > 0$ , independent of  $h$ , such that*

$$C \|\boldsymbol{\tau}_h\|_{\mathbf{div};\Omega}^2 \leq \|\boldsymbol{\tau}_{0h}\|_{\mathbf{div};\Omega}^2 \quad \forall \boldsymbol{\tau}_h \in \mathbf{V}_h. \quad (3.8)$$

**Proof.** Given  $\boldsymbol{\tau}_h = \boldsymbol{\tau}_{0h} + d_h \mathbf{I} \in \mathbf{V}_h$ , with  $\boldsymbol{\tau}_{0h} \in H_{0,h} := H_h \cap \mathbb{H}_0(\mathbf{div}; \Omega)$  and  $d_h \in \mathbb{R}$ , we have that

$$0 = \langle \boldsymbol{\tau}_h \boldsymbol{\nu}, \tilde{\boldsymbol{\lambda}} \rangle_{\Gamma_N} = \langle \boldsymbol{\tau}_{0h} \boldsymbol{\nu}, \tilde{\boldsymbol{\lambda}} \rangle_{\Gamma_N} + d_h \langle \boldsymbol{\nu}, \tilde{\boldsymbol{\lambda}} \rangle_{\Gamma_N},$$

which yields,  $d_h = -\frac{\langle \boldsymbol{\tau}_{0h} \boldsymbol{\nu}, \tilde{\boldsymbol{\lambda}} \rangle_{\Gamma_N}}{\langle \boldsymbol{\nu}, \tilde{\boldsymbol{\lambda}} \rangle_{\Gamma_N}}$ . Hence, by continuity of the normal trace operator we find that

$$|d_h| \leq \tilde{C} \frac{\|\tilde{\boldsymbol{\lambda}}\|_{0;1/2,\Gamma_N}}{|\langle \boldsymbol{\nu}, \tilde{\boldsymbol{\lambda}} \rangle_{\Gamma_N}|} \|\boldsymbol{\tau}_{0h}\|_{\mathbf{div};\Omega},$$

which, together with the fact that  $\|\boldsymbol{\tau}_h\|_{\mathbf{div};\Omega}^2 = \|\boldsymbol{\tau}_{0h}\|_{\mathbf{div};\Omega}^2 + 2|\Omega| |d_h|^2$ , implies (3.8).  $\square$

Now concerning the existence of  $\tilde{\boldsymbol{\lambda}} \in \mathbf{H}_{00}^{1/2}(\Gamma_N)$  such that  $\tilde{\boldsymbol{\lambda}} \in Q_h$  for all  $h > 0$  and  $\langle \boldsymbol{\nu}, \tilde{\boldsymbol{\lambda}} \rangle_{\Gamma_N} \neq 0$ , we may proceed as in [27, Section 3.2]. Indeed, we pick one corner point of  $\Gamma_N$  and define a function  $v$  that is continuous, linear on each side of  $\Gamma_N$ , equal to one in the chosen vertex and zero on all other ones. If  $\boldsymbol{\nu}_1$  and  $\boldsymbol{\nu}_2$  are the normal vectors on the two sides of  $\Gamma_N$  that meet at the corner point, then  $\tilde{\boldsymbol{\lambda}} := v(\boldsymbol{\nu}_1 + \boldsymbol{\nu}_2)$  satisfies the required property. If  $\Gamma_N$  has no corner point then we just take any interior point of  $\Gamma_N$  that is a vertex of all the partitions of  $\Gamma_N$  defining  $Q_h$  and proceed as before.

Now, we are in a position to show the  $\mathbf{V}_h$ -ellipticity of the bilinear form  $a$ .

**Lemma 3.4** *There exists  $c > 0$ , depending only on  $\Gamma_N$  and  $\Omega$ , such that*

$$a(\boldsymbol{\tau}_h, \boldsymbol{\tau}_h) \geq c \|\boldsymbol{\tau}_h\|_{\mathbf{div};\Omega}^2 \quad \forall \boldsymbol{\tau}_h \in \mathbf{V}_h.$$

**Proof.** Given  $\boldsymbol{\tau}_h = \boldsymbol{\tau}_{0h} + d_h \mathbf{I} \in \mathbf{V}_h$ , with  $\boldsymbol{\tau}_{0h} \in H_{0,h} := H_h \cap \mathbb{H}_0(\mathbf{div}; \Omega)$  and  $d_h \in \mathbb{R}$ , we apply Lemmas 2.2 and 3.3 to deduce that

$$\begin{aligned} a(\boldsymbol{\tau}_h, \boldsymbol{\tau}_h) &= \frac{1}{\mu} \|\boldsymbol{\tau}_h\|_{0,\Omega}^2 + \frac{1}{\alpha} \|\mathbf{div} \boldsymbol{\tau}_h\|_{0,\Omega}^2 \\ &\geq \delta_1 C_1 \|\boldsymbol{\tau}_{0h}\|_{0,\Omega}^2 + \frac{1}{2\alpha} \|\mathbf{div} \boldsymbol{\tau}_{0h}\|_{0,\Omega}^2 \\ &\geq \delta_2 \|\boldsymbol{\tau}_{0h}\|_{\mathbf{div};\Omega}^2 \geq \delta_2 C \|\boldsymbol{\tau}_h\|_{\mathbf{div};\Omega}^2, \end{aligned}$$

where  $\delta_1 := \min \left\{ \frac{1}{\mu}, \frac{1}{2\alpha} \right\}$  and  $\delta_2 := \min \left\{ \delta_1 C_1, \frac{1}{2\alpha} \right\}$ , which completes the proof.  $\square$

The following theorem establishes the well posedness of (3.5) and the associated Cea estimate.

**Theorem 3.1** *Let  $Q_h$  be any of the two choices described above with the conditions assumed in and derived from Lemmas 3.1 and 3.2. Then the Galerkin scheme (3.5) has a unique solution  $(\boldsymbol{\sigma}_h, \boldsymbol{\xi}_h) \in H_h \times Q_h$  and there exist positive constants  $C, \tilde{C}$ , independent of  $h$ , such that*

$$\|(\boldsymbol{\sigma}_h, \boldsymbol{\xi}_h)\|_{H \times Q} \leq C \left\{ \|\mathbf{f}\|_{0,\Omega} + \|\mathbf{g}\|_{-1/2,\Gamma_N} \right\},$$

and

$$\|(\boldsymbol{\sigma}, \boldsymbol{\xi}) - (\boldsymbol{\sigma}_h, \boldsymbol{\xi}_h)\|_{H \times Q} \leq \tilde{C} \inf_{(\boldsymbol{\tau}_h, \boldsymbol{\lambda}_h) \in H_h \times Q_h} \|(\boldsymbol{\sigma}, \boldsymbol{\xi}) - (\boldsymbol{\tau}_h, \boldsymbol{\lambda}_h)\|_{H \times Q}. \quad (3.9)$$

**Proof.** Thanks to the previous results given by Lemmas 3.1, 3.2, and 3.4, the proof follows from a direct application of the discrete Babuška-Brezzi theory (see, e.g. [28, Theorem 1.1, Chapter II] or [7, Chapter II]).  $\square$

In order to provide the rate of convergence of the Galerkin scheme (3.5), we need to introduce the Raviart-Thomas interpolation operator (see [7], [33])  $\Pi_h^k : \mathbb{H}^1(\Omega) \rightarrow H_h$ , which, given  $\boldsymbol{\tau} \in \mathbb{H}^1(\Omega)$ , is characterized by the following identities:

$$\int_e \Pi_h^k(\boldsymbol{\tau}) \boldsymbol{\nu} \cdot \mathbf{p} = \int_e \boldsymbol{\tau} \boldsymbol{\nu} \cdot \mathbf{p} \quad \forall \text{ edge } e \in \mathcal{T}_h, \quad \forall \mathbf{p} \in \mathbf{P}_k(e), \quad \text{when } k \geq 0. \quad (3.10)$$

and

$$\int_T \Pi_h^k(\boldsymbol{\tau}) : \boldsymbol{\rho} = \int_T \boldsymbol{\tau} : \boldsymbol{\rho} \quad \forall T \in \mathcal{T}_h, \quad \forall \boldsymbol{\rho} \in \mathbb{P}_{k-1}(T), \quad \text{when } k \geq 1. \quad (3.11)$$

Recall, according to the notations introduced in Section 1, that  $\mathbf{P}_k(e) := [P_k(e)]^2$  and  $\mathbb{P}_{k-1}(T) := [P_{k-1}(T)]^{2 \times 2}$ . Then, it is easy to show, using (3.10) and (3.11), that

$$\mathbf{div}(\Pi_h^k(\boldsymbol{\tau})) = \mathcal{P}_h^k(\mathbf{div} \boldsymbol{\tau}), \quad (3.12)$$

where  $\mathcal{P}_h^k : \mathbf{L}^2(\Omega) \rightarrow \mathcal{Q}_h^{\mathbf{u}}$  is the  $\mathbf{L}^2(\Omega)$  - orthogonal projector. It is well known (see, e.g. [15]) that for each  $\mathbf{v} \in \mathbf{H}^m(\Omega)$ , with  $0 \leq m \leq k+1$ , there holds

$$\|\mathbf{v} - \mathcal{P}_h^k(\mathbf{v})\|_{0,T} \leq C h_T^m |\mathbf{v}|_{m,T} \quad \forall T \in \mathcal{T}_h. \quad (3.13)$$

In addition, the operator  $\Pi_h^k$  satisfies the following approximation properties (see, e.g. [7], [33]):

$$\|\boldsymbol{\tau} - \Pi_h^k(\boldsymbol{\tau})\|_{0,T} \leq C h_T^m |\boldsymbol{\tau}|_{m,T} \quad \forall T \in \mathcal{T}_h, \quad (3.14)$$

for each  $\boldsymbol{\tau} \in \mathbb{H}^m(\Omega)$ , with  $1 \leq m \leq k+1$ ,

$$\|\mathbf{div}(\boldsymbol{\tau} - \Pi_h^k(\boldsymbol{\tau}))\|_{0,T} \leq C h_T^m |\mathbf{div}(\boldsymbol{\tau})|_{m,T} \quad \forall T \in \mathcal{T}_h, \quad (3.15)$$

for each  $\boldsymbol{\tau} \in \mathbb{H}^1(\Omega)$  such that  $\mathbf{div}(\boldsymbol{\tau}) \in \mathbf{H}^m(\Omega)$ , with  $0 \leq m \leq k+1$ , and

$$\|\boldsymbol{\tau} \boldsymbol{\nu} - \Pi_h^k(\boldsymbol{\tau}) \boldsymbol{\nu}\|_{0,e} \leq C h_e^{1/2} \|\boldsymbol{\tau}\|_{1,T_e} \quad \forall \text{edge } e \in \mathcal{T}_h, \quad (3.16)$$

for each  $\boldsymbol{\tau} \in \mathbb{H}^1(\Omega)$ , where  $T_e \in \mathcal{T}_h$  contains  $e$  on its boundary. In particular, note that (3.15) follows easily from (3.12) and (3.13). Moreover, the interpolation operator  $\Pi_h^k$  can also be defined as a bounded linear operator from the larger space  $\mathbb{H}^s(\Omega) \cap \mathbb{H}(\mathbf{div}; \Omega)$  into  $H_h$  for all  $s \in (0, 1]$  (see, e.g. [30, Theorem 3.16]), and in this case there holds the following interpolation error estimate

$$\|\boldsymbol{\tau} - \Pi_h^k(\boldsymbol{\tau})\|_{0,T} \leq C h_T^s \left\{ \|\boldsymbol{\tau}\|_{s,T} + \|\mathbf{div}(\boldsymbol{\tau})\|_{0,T} \right\} \quad \forall T \in \mathcal{T}_h. \quad (3.17)$$

Then, as a consequence of (3.17), (3.13), (3.14), (3.15), (3.16), and the usual interpolation estimates, we find that  $H_h$  and  $Q_h$  satisfy the following approximation properties:

**(AP $_h^\sigma$ )** For each  $s \in (0, k+1]$  and for each  $\boldsymbol{\tau} \in \mathbb{H}^s(\Omega)$  with  $\mathbf{div}(\boldsymbol{\tau}) \in \mathbf{H}^s(\Omega)$  there exists  $\boldsymbol{\tau}_h \in H_h$  such that

$$\|\boldsymbol{\tau} - \boldsymbol{\tau}_h\|_{\mathbf{div}, \Omega} \leq C h^s \left\{ \|\boldsymbol{\tau}\|_{s, \Omega} + \|\mathbf{div}(\boldsymbol{\tau})\|_{s, \Omega} \right\}.$$

**(AP $_h^\xi$ )** For each  $s \in [0, k+1]$  and for each  $\boldsymbol{\lambda} \in \mathbf{H}_{00}^{s+1/2}(\Gamma_N)$ , there exists  $\boldsymbol{\lambda}_h \in Q_h$  such that

$$\|\boldsymbol{\lambda} - \boldsymbol{\lambda}_h\|_{0;1/2, \Gamma_N} \leq C h^s \|\boldsymbol{\lambda}\|_{s+1/2, \Gamma_N}.$$

The following theorem provides the theoretical rate of convergence of the Galerkin scheme (3.5), under suitable regularity assumptions on the exact solution.

**Theorem 3.2** *Let  $(\boldsymbol{\sigma}, \boldsymbol{\xi}) \in H \times Q$  and  $(\boldsymbol{\sigma}_h, \boldsymbol{\xi}_h) \in H_h \times Q_h$  be the unique solutions of the continuous and discrete formulations (2.7) and (3.5), respectively. Assume that  $\boldsymbol{\sigma} \in \mathbb{H}^s(\Omega)$ ,  $\mathbf{div}(\boldsymbol{\sigma}) \in \mathbf{H}^s(\Omega)$  and  $\boldsymbol{\xi} \in \mathbf{H}_{00}^{s+1/2}(\Gamma_N)$ , for some  $s \in (0, k+1]$ . Then, there exists  $C > 0$ , independent of  $h$ , such that*

$$\|(\boldsymbol{\sigma}, \boldsymbol{\xi}) - (\boldsymbol{\sigma}_h, \boldsymbol{\xi}_h)\|_{H \times Q} \leq C h^s \left\{ \|\boldsymbol{\sigma}\|_{s, \Omega} + \|\mathbf{div}(\boldsymbol{\sigma})\|_{s, \Omega} + \|\boldsymbol{\xi}\|_{s+1/2, \Gamma_N} \right\}.$$

**Proof.** It is a straightforward consequence of the Cea estimate (3.9) and the approximation properties **(AP $_h^\sigma$ )** and **(AP $_h^\xi$ )**. □

## 4 A residual-based a posteriori error estimator

In this section we develop a residual-based a-posteriori error analysis for the mixed finite element scheme (3.5).

### 4.1 Preliminaries

First we introduce several notations. Given  $T \in \mathcal{T}_h$ , we let  $\mathcal{E}(T)$  be the set of its edges, and let  $\mathcal{E}_h$  be the set of all edges of the triangulation  $\mathcal{T}_h$ . Then we write  $\mathcal{E}_h = \mathcal{E}_h(\Omega) \cup \mathcal{E}_h(\Gamma_D) \cup \mathcal{E}_h(\Gamma_N)$ , where  $\mathcal{E}_h(\Omega) := \{e \in \mathcal{E}_h : e \subseteq \Omega\}$ ,  $\mathcal{E}_h(\Gamma_D) := \{e \in \mathcal{E}_h : e \subseteq \Gamma_D\}$  and  $\mathcal{E}_h(\Gamma_N) := \{e \in \mathcal{E}_h : e \subseteq \Gamma_N\}$ . Also, for each edge  $e \in \mathcal{E}_h$  we fix a unit normal vector  $\boldsymbol{\nu}_e := (\nu_1, \nu_2)^t$ , and let  $\mathbf{s}_e := (-\nu_2, \nu_1)^t$  be the corresponding fixed unit tangential vector along  $e$ . Then, given  $e \in \mathcal{E}_h(\Omega)$  and  $\boldsymbol{\tau} \in \mathbb{L}^2(\Omega)$  such that  $\boldsymbol{\tau}|_T \in \mathbb{C}(T)$  on each  $T \in \mathcal{T}_h$ , we let  $[\boldsymbol{\tau} \mathbf{s}_e]$  be the corresponding jump across  $e$ , that is,  $[\boldsymbol{\tau} \mathbf{s}_e] := (\boldsymbol{\tau}|_T - \boldsymbol{\tau}|_{T'})|_e \mathbf{s}_e$ , where  $T$  and  $T'$  are the triangles of  $\mathcal{T}_h$  having  $e$  as a common edge. Abusing notation, when  $e \in \mathcal{E}_h(\Gamma)$ , we also write  $[\boldsymbol{\tau} \mathbf{s}_e] := \boldsymbol{\tau}|_e \mathbf{s}_e$ . From now on, when no confusion arises, we simply write  $\mathbf{s}$  and  $\boldsymbol{\nu}$  instead of  $\mathbf{s}_e$  and  $\boldsymbol{\nu}_e$ , respectively. Finally, given scalar, vector and tensor valued fields  $v$ ,  $\boldsymbol{\varphi} := (\varphi_1, \varphi_2)$  and  $\boldsymbol{\tau} := (\tau_{ij})$ , respectively, we let

$$\mathbf{curl}(v) := \begin{pmatrix} \frac{\partial v}{\partial x_2} \\ -\frac{\partial v}{\partial x_1} \end{pmatrix}, \quad \underline{\mathbf{curl}}(\varphi) := \begin{pmatrix} \mathbf{curl}(\varphi_1)^t \\ \mathbf{curl}(\varphi_2)^t \end{pmatrix}, \quad \text{and } \mathbf{curl}(\boldsymbol{\tau}) := \begin{pmatrix} \frac{\partial \tau_{12}}{\partial x_1} - \frac{\partial \tau_{11}}{\partial x_2} \\ \frac{\partial \tau_{22}}{\partial x_1} - \frac{\partial \tau_{21}}{\partial x_2} \end{pmatrix}.$$

Then, letting  $(\boldsymbol{\sigma}, \boldsymbol{\xi}) \in H \times Q$  and  $(\boldsymbol{\sigma}_h, \boldsymbol{\xi}_h) \in H_h \times Q_h$  be the unique solutions of the continuous and discrete formulations (2.7) and (3.5), respectively, we define for each  $T \in \mathcal{T}_h$  a local error indicator  $\theta_T$  as follows:

$$\begin{aligned} \theta_T^2 := & \|\mathbf{f} - \mathcal{P}_h^k(\mathbf{f})\|_{0,T}^2 + h_T^2 \left\| \frac{1}{\mu} \boldsymbol{\sigma}_h^d - \nabla \mathbf{u}_h \right\|_{0,T}^2 + \frac{h_T^2}{\mu^2} \|\mathbf{curl}(\boldsymbol{\sigma}_h^d)\|_{0,T}^2 \\ & + \sum_{e \in \mathcal{E}(T) \cap \mathcal{E}_h(\Omega)} \frac{h_e}{\mu^2} \|[(\boldsymbol{\sigma}_h^d) \mathbf{s}]\|_{0,e}^2 + \sum_{e \in \mathcal{E}(T) \cap \mathcal{E}_h(\Gamma_D)} \frac{h_e}{\mu^2} \|(\boldsymbol{\sigma}_h^d) \mathbf{s}\|_{0,e}^2 \\ & + \sum_{e \in \mathcal{E}(T) \cap \mathcal{E}_h(\Gamma_N)} h_e \left\{ \left\| \left( \frac{1}{\mu} \boldsymbol{\sigma}_h^d \right) \mathbf{s} + \frac{d\boldsymbol{\xi}_h}{ds} \right\|_{0,e}^2 + \|\boldsymbol{\xi}_h + \mathbf{u}_h\|_{0,e}^2 + \|\mathbf{g} - \boldsymbol{\sigma}_h \boldsymbol{\nu}\|_{0,e}^2 \right\}, \end{aligned} \quad (4.1)$$

where, resembling (2.5), we set

$$\mathbf{u}_h := \frac{1}{\alpha} \left\{ \mathcal{P}_h^k(\mathbf{f}) + \mathbf{div}(\boldsymbol{\sigma}_h) \right\} \quad \text{in } \Omega. \quad (4.2)$$

Note that the last term defining  $\theta_T^2$  requires that  $\mathbf{g}|_e \in \mathbf{L}^2(e) \quad \forall e \in \mathcal{E}_h(\Gamma_N)$ . The residual character of each term on the right hand side of (4.1) is quite clear. As usual the expression

$$\boldsymbol{\theta} := \left\{ \sum_{T \in \mathcal{T}_h} \theta_T^2 \right\}^{1/2} \quad (4.3)$$

is employed as the global residual error estimator.

The following theorem constitutes the main result of this section.

**Theorem 4.1** *Let  $(\boldsymbol{\sigma}, \boldsymbol{\xi}) \in H \times Q$  and  $(\boldsymbol{\sigma}_h, \boldsymbol{\xi}_h) \in H_h \times Q_h$  be the unique solutions of (2.7) and (3.5), respectively. In addition, let  $\mathbf{u} \in \mathbf{L}^2(\Omega)$  be defined according to (2.5), that is  $\mathbf{u} := \frac{1}{\alpha} \{\mathbf{f} + \mathbf{div}(\boldsymbol{\sigma})\}$ , and assume that the Neumann datum  $\mathbf{g}$  belongs to  $\mathbf{L}^2(\Gamma_N)$ . Then, there exist positive constants  $C_{\text{eff}}$  and  $C_{\text{rel}}$ , independent of  $h$ , such that*

$$C_{\text{eff}} \boldsymbol{\theta} + h.o.t. \leq \|\mathbf{u} - \mathbf{u}_h\|_{0,\Omega} + \|(\boldsymbol{\sigma} - \boldsymbol{\sigma}_h, \boldsymbol{\xi} - \boldsymbol{\xi}_h)\|_{H \times Q} \leq C_{\text{rel}} \boldsymbol{\theta}. \quad (4.4)$$

where *h.o.t.* stands for one or several terms of higher order.

The proof of Theorem 4.1 is separated into the two parts given by the next subsections. The efficiency of the global error estimator (lower bound in 4.4) is proved below in Section 4.3, whereas the corresponding reliability (upper bound in 4.4) is derived next.

## 4.2 Reliability

We begin with the following preliminary estimate.

**Lemma 4.1** *Let  $(\boldsymbol{\sigma}, \boldsymbol{\xi}) \in H \times Q$  and  $(\boldsymbol{\sigma}_h, \boldsymbol{\xi}_h) \in H_h \times Q_h$  be the unique solutions of (2.7) and (3.5), respectively. Then there exists  $C > 0$ , independent of  $h$ , such that*

$$C \|(\boldsymbol{\sigma} - \boldsymbol{\sigma}_h, \boldsymbol{\xi} - \boldsymbol{\xi}_h)\|_{H \times Q} \leq \sup_{\substack{\boldsymbol{\tau} \in H \\ \boldsymbol{\tau} \neq \mathbf{0}}} \frac{|E(\boldsymbol{\tau})|}{\|\boldsymbol{\tau}\|_{\mathbf{div};\Omega}} + \|\mathbf{g} - \boldsymbol{\sigma}_h \boldsymbol{\nu}\|_{-1/2,\Gamma_N}, \quad (4.5)$$

where, given any  $\boldsymbol{\tau}_h \in H_h$ ,

$$E(\boldsymbol{\tau}) := \langle (\boldsymbol{\tau} - \boldsymbol{\tau}_h) \boldsymbol{\nu}, \boldsymbol{\xi}_h \rangle_{\Gamma_N} + \frac{1}{\mu} \int_{\Omega} \boldsymbol{\sigma}_h^d : (\boldsymbol{\tau} - \boldsymbol{\tau}_h) + \frac{1}{\alpha} \int_{\Omega} (\mathbf{f} + \mathbf{div}(\boldsymbol{\sigma}_h)) \cdot \mathbf{div}(\boldsymbol{\tau} - \boldsymbol{\tau}_h). \quad (4.6)$$

**Proof.** We first observe from Theorem 2.1 that the bounded linear operator  $\mathcal{A} : H \times Q \rightarrow (H \times Q)' \equiv H' \times Q'$ , which is induced by the left-hand side of the equations in (2.7), is an isomorphism. This means, in particular, that there exists  $C > 0$  such that

$$\|\mathcal{A}(\boldsymbol{\rho}, \boldsymbol{\zeta})\|_{H' \times Q'} \geq C \|(\boldsymbol{\rho}, \boldsymbol{\zeta})\|_{H \times Q} \quad \forall (\boldsymbol{\rho}, \boldsymbol{\zeta}) \in H \times Q,$$

which can be written, equivalently, as

$$C \|(\boldsymbol{\rho}, \boldsymbol{\zeta})\|_{H \times Q} \leq \sup_{\substack{(\boldsymbol{\tau}, \boldsymbol{\lambda}) \in H \times Q \\ (\boldsymbol{\tau}, \boldsymbol{\lambda}) \neq (\mathbf{0}, \mathbf{0})}} \frac{a(\boldsymbol{\rho}, \boldsymbol{\tau}) + b(\boldsymbol{\tau}, \boldsymbol{\zeta}) + b(\boldsymbol{\rho}, \boldsymbol{\lambda})}{\|(\boldsymbol{\tau}, \boldsymbol{\lambda})\|_{H \times Q}} \quad \forall (\boldsymbol{\rho}, \boldsymbol{\zeta}) \in H \times Q.$$

In particular, for the Galerkin error  $(\boldsymbol{\rho}, \boldsymbol{\zeta}) = (\boldsymbol{\sigma} - \boldsymbol{\sigma}_h, \boldsymbol{\xi} - \boldsymbol{\xi}_h)$ , we obtain

$$\begin{aligned} C \|(\boldsymbol{\sigma} - \boldsymbol{\sigma}_h, \boldsymbol{\xi} - \boldsymbol{\xi}_h)\|_{H \times Q} &\leq \sup_{\substack{(\boldsymbol{\tau}, \boldsymbol{\lambda}) \in H \times Q \\ (\boldsymbol{\tau}, \boldsymbol{\lambda}) \neq (\mathbf{0}, \mathbf{0})}} \frac{a(\boldsymbol{\sigma} - \boldsymbol{\sigma}_h, \boldsymbol{\tau}) + b(\boldsymbol{\tau}, \boldsymbol{\xi} - \boldsymbol{\xi}_h) + b(\boldsymbol{\sigma} - \boldsymbol{\sigma}_h, \boldsymbol{\lambda})}{\|(\boldsymbol{\tau}, \boldsymbol{\lambda})\|_{H \times Q}} \\ &\leq \sup_{\substack{(\boldsymbol{\tau}, \boldsymbol{\lambda}) \in H \times Q \\ (\boldsymbol{\tau}, \boldsymbol{\lambda}) \neq (\mathbf{0}, \mathbf{0})}} \left\{ \frac{a(\boldsymbol{\sigma} - \boldsymbol{\sigma}_h, \boldsymbol{\tau}) + b(\boldsymbol{\tau}, \boldsymbol{\xi} - \boldsymbol{\xi}_h)}{\|\boldsymbol{\tau}\|_{\mathbf{div}; \Omega}} + \frac{b(\boldsymbol{\sigma} - \boldsymbol{\sigma}_h, \boldsymbol{\lambda})}{\|\boldsymbol{\lambda}\|_{0; 1/2, \Gamma_N}} \right\} \\ &\leq \sup_{\substack{\boldsymbol{\tau} \in H \\ \boldsymbol{\tau} \neq \mathbf{0}}} \frac{\tilde{E}(\boldsymbol{\tau})}{\|\boldsymbol{\tau}\|_{\mathbf{div}; \Omega}} + \sup_{\substack{\boldsymbol{\lambda} \in Q \\ \boldsymbol{\lambda} \neq \mathbf{0}}} \frac{b(\boldsymbol{\sigma} - \boldsymbol{\sigma}_h, \boldsymbol{\lambda})}{\|\boldsymbol{\lambda}\|_{0; 1/2, \Gamma_N}}, \end{aligned}$$

where  $\tilde{E}(\boldsymbol{\tau}) := a(\boldsymbol{\sigma} - \boldsymbol{\sigma}_h, \boldsymbol{\tau}) + b(\boldsymbol{\tau}, \boldsymbol{\xi} - \boldsymbol{\xi}_h)$ . But, from the second equation of (2.7) and the definition of the bilinear form  $b$ , we see that  $b(\boldsymbol{\sigma} - \boldsymbol{\sigma}_h, \boldsymbol{\lambda}) = \langle \mathbf{g} - \boldsymbol{\sigma}_h \boldsymbol{\nu}, \boldsymbol{\lambda} \rangle_{\Gamma_N}$ , which yields

$$\sup_{\substack{\boldsymbol{\lambda} \in Q \\ \boldsymbol{\lambda} \neq \mathbf{0}}} \frac{b(\boldsymbol{\sigma} - \boldsymbol{\sigma}_h, \boldsymbol{\lambda})}{\|\boldsymbol{\lambda}\|_{0; 1/2, \Gamma_N}} = \sup_{\substack{\boldsymbol{\lambda} \in Q \\ \boldsymbol{\lambda} \neq \mathbf{0}}} \frac{\langle \mathbf{g} - \boldsymbol{\sigma}_h \boldsymbol{\nu}, \boldsymbol{\lambda} \rangle_{\Gamma_N}}{\|\boldsymbol{\lambda}\|_{0; 1/2, \Gamma_N}} = \|\mathbf{g} - \boldsymbol{\sigma}_h \boldsymbol{\nu}\|_{-1/2, \Gamma_N}.$$

Next, we observe from the first equations of (2.7) and (3.5) that

$$a(\boldsymbol{\sigma}, \boldsymbol{\tau}) + b(\boldsymbol{\tau}, \boldsymbol{\xi}) = F(\boldsymbol{\tau}) \quad \forall \boldsymbol{\tau} \in H \quad \text{and} \quad a(\boldsymbol{\sigma}_h, \boldsymbol{\tau}_h) + b(\boldsymbol{\tau}_h, \boldsymbol{\xi}_h) = F(\boldsymbol{\tau}_h) \quad \forall \boldsymbol{\tau}_h \in H_h,$$

where  $F(\boldsymbol{\tau}) := -\frac{1}{\alpha} \int_{\Omega} \mathbf{f} \cdot \mathbf{div}(\boldsymbol{\tau}) \quad \forall \boldsymbol{\tau} \in H$ . It follows that

$$\tilde{E}(\boldsymbol{\tau}) = F(\boldsymbol{\tau}) - a(\boldsymbol{\sigma}_h, \boldsymbol{\tau}) - b(\boldsymbol{\tau}, \boldsymbol{\xi}_h) \quad \forall \boldsymbol{\tau} \in H$$

and

$$\tilde{E}(\boldsymbol{\tau}_h) = 0 \quad \forall \boldsymbol{\tau}_h \in H_h,$$

whence

$$\tilde{E}(\boldsymbol{\tau}) = \tilde{E}(\boldsymbol{\tau}) - \tilde{E}(\boldsymbol{\tau}_h) = \tilde{E}(\hat{\boldsymbol{\tau}}) \quad \forall \boldsymbol{\tau} \in H,$$

where  $\widehat{\boldsymbol{\tau}} := \boldsymbol{\tau} - \boldsymbol{\tau}_h$ . In this way, it is easy to see, according to the definitions of  $F$ ,  $a$  and  $b$ , that the above expression for  $\widetilde{E}$  leads to (4.6) with  $E = -\widetilde{E}$ , thus completing the proof.  $\square$

We now aim to bound the supremum on the right hand side of (4.5), for which we need a suitable choice of  $\boldsymbol{\tau}_h \in H_h$ . To this end, we will use the Clément interpolation operator  $I_h : H^1(\Omega) \rightarrow X_h$  (cf. [16]), where

$$X_h := \{v \in C(\bar{\Omega}) : v|_T \in P_1(T) \quad \forall T \in \mathcal{T}_h\}.$$

A vectorial version of  $I_h$ , say  $\mathbf{I}_h : \mathbf{H}^1(\Omega) \rightarrow \mathbf{X}_h$ , which is defined componentwise by  $I_h$ , is also required. The following lemma establishes the local approximation properties of  $I_h$ .

**Lemma 4.2** *There exist constants  $c_1, c_2 > 0$ , independent of  $h$ , such that for all  $v \in H^1(\Omega)$  there holds*

$$\|v - I_h(v)\|_{0,T} \leq c_1 h_T \|v\|_{1,\Delta(T)} \quad \forall T \in \mathcal{T}_h,$$

and

$$\|v - I_h(v)\|_{0,e} \leq c_2 h_e^{1/2} \|v\|_{1,\Delta(e)} \quad \forall e \in \mathcal{E}_h,$$

where  $\Delta(T) := \cup\{T' \in \mathcal{T}_h : T' \cap T \neq \emptyset\}$  and  $\Delta(e) := \cup\{T' \in \mathcal{T}_h : T' \cap e \neq \emptyset\}$ .

**Proof.** See [16].  $\square$

Next, for each  $\boldsymbol{\tau} \in H$  we consider its Helmholtz decomposition

$$\boldsymbol{\tau} = \underline{\mathbf{curl}}(\boldsymbol{\chi}) + \nabla \mathbf{z},$$

where  $\boldsymbol{\chi} \in \mathbf{H}^1(\Omega)$  and  $\mathbf{z} \in \mathbf{H}^2(\Omega)$  satisfy  $\Delta \mathbf{z} = \operatorname{div} \boldsymbol{\tau}$  in  $\Omega$ , and

$$\|\boldsymbol{\chi}\|_{1,\Omega} + \|\mathbf{z}\|_{2,\Omega} \leq C \|\boldsymbol{\tau}\|_{\operatorname{div};\Omega}. \quad (4.7)$$

Then, we let  $\boldsymbol{\chi}_h := \mathbf{I}_h(\boldsymbol{\chi})$  and define

$$\boldsymbol{\tau}_h := \Pi_h^k(\boldsymbol{\zeta}) + \underline{\mathbf{curl}}(\boldsymbol{\chi}_h) \in H_h, \quad (4.8)$$

where  $\boldsymbol{\zeta} := \nabla \mathbf{z} \in \mathbb{H}^1(\Omega)$  and  $\Pi_h^k$  is the the Raviart-Thomas interpolation operator introduced before (cf. (3.10) and (3.11)). We refer to (4.8) as a discrete Helmholtz decomposition of  $\boldsymbol{\tau}_h$ . Therefore, we can write

$$\widehat{\boldsymbol{\tau}} := \boldsymbol{\tau} - \Pi_h^k(\boldsymbol{\zeta}) - \underline{\mathbf{curl}}(\boldsymbol{\chi}_h) = \boldsymbol{\zeta} - \Pi_h^k(\boldsymbol{\zeta}) + \underline{\mathbf{curl}}(\boldsymbol{\chi} - \boldsymbol{\chi}_h), \quad (4.9)$$

which, using (3.12) and the fact that  $\operatorname{div} \boldsymbol{\zeta} = \Delta \mathbf{z} = \operatorname{div} \boldsymbol{\tau}$  in  $\Omega$ , yields

$$\operatorname{div}(\widehat{\boldsymbol{\tau}}) = \operatorname{div}(\boldsymbol{\zeta} - \Pi_h^k(\boldsymbol{\zeta})) = (\mathbf{I} - \mathcal{P}_h^k)(\operatorname{div}(\boldsymbol{\zeta})) = (\mathbf{I} - \mathcal{P}_h^k)(\operatorname{div}(\boldsymbol{\tau})). \quad (4.10)$$

Hence, replacing (4.9) and (4.10) into (4.6), we find that

$$E(\boldsymbol{\tau}) = E_1(\boldsymbol{\tau}) + E_2(\boldsymbol{\zeta}) + E_3(\boldsymbol{\chi}), \quad (4.11)$$

where

$$E_1(\boldsymbol{\tau}) := \frac{1}{\alpha} \int_{\Omega} (\mathbf{f} + \operatorname{div}(\boldsymbol{\sigma}_h)) \cdot (\mathbf{I} - \mathcal{P}_h^k)(\operatorname{div}(\boldsymbol{\tau})), \quad (4.12)$$

$$E_2(\boldsymbol{\zeta}) := \int_{\Omega} \frac{1}{\mu} \boldsymbol{\sigma}_h^{\mathbf{d}} : (\boldsymbol{\zeta} - \Pi_h^k(\boldsymbol{\zeta})) + \langle (\boldsymbol{\zeta} - \Pi_h^k(\boldsymbol{\zeta})) \boldsymbol{\nu}, \boldsymbol{\xi}_h \rangle_{\Gamma_N},$$

and

$$E_3(\boldsymbol{\chi}) := \int_{\Omega} \frac{1}{\mu} \boldsymbol{\sigma}_h^{\mathbf{d}} : \underline{\mathbf{curl}}(\boldsymbol{\chi} - \boldsymbol{\chi}_h) + \langle \underline{\mathbf{curl}}(\boldsymbol{\chi} - \boldsymbol{\chi}_h) \boldsymbol{\nu}, \boldsymbol{\xi}_h \rangle_{\Gamma_N}. \quad (4.13)$$

The following three lemmas provide the upper bounds for  $|E_1(\boldsymbol{\tau})|$ ,  $|E_2(\boldsymbol{\zeta})|$ , and  $|E_3(\boldsymbol{\chi})|$ .

**Lemma 4.3** *There holds*

$$|E_1(\boldsymbol{\tau})| \leq \frac{1}{\alpha} \left\{ \sum_{T \in \mathcal{T}_h} \|\mathbf{f} - \mathcal{P}_h^k(\mathbf{f})\|_{0,T}^2 \right\}^{1/2} \|\mathbf{div}(\boldsymbol{\tau})\|_{0,\Omega}.$$

**Proof.** Since  $\mathbf{div}(\boldsymbol{\sigma}_h)$  belong to  $\mathcal{Q}_h^{\mathbf{u}}$  (cf. (3.2)), and  $\mathcal{P}_h^k$  is precisely the orthogonal projector onto  $\mathcal{Q}_h^{\mathbf{u}}$ , we obtain from the first equation of (4.12) that

$$E_1(\boldsymbol{\tau}) = \frac{1}{\alpha} \int_{\Omega} \mathbf{f} \cdot (\mathbf{I} - \mathcal{P}_h^k)(\mathbf{div}(\boldsymbol{\tau})) = \frac{1}{\alpha} \int_{\Omega} (\mathbf{I} - \mathcal{P}_h^k)(\mathbf{f}) \cdot \mathbf{div}(\boldsymbol{\tau}).$$

Thus, a simple application of the Cauchy-Schwarz inequality completes the proof.  $\square$

**Lemma 4.4** *There exists  $C > 0$ , independent of  $\mu$  and  $\alpha$ , such that*

$$|E_2(\boldsymbol{\zeta})| \leq C \left\{ \sum_{T \in \mathcal{T}_h} h_T^2 \left\| \frac{1}{\mu} \boldsymbol{\sigma}_h^{\mathbf{d}} - \nabla \mathbf{u}_h \right\|_{0,T}^2 + \sum_{e \in \mathcal{E}_h(\Gamma_N)} h_e \|\boldsymbol{\xi}_h + \mathbf{u}_h\|_{0,e}^2 \right\}^{1/2} \|\boldsymbol{\tau}\|_{\mathbf{div};\Omega}.$$

**Proof.** Since  $\boldsymbol{\zeta} \in \mathbb{H}^1(\Omega)$ , it follows that  $(\boldsymbol{\zeta} - \Pi_h^k(\boldsymbol{\zeta})) \boldsymbol{\nu}|_{\Gamma_N}$  belongs to  $\mathbf{L}^2(\Gamma_N)$ , whence  $E_2(\boldsymbol{\zeta})$  (cf. (4.12)) can be redefined as:

$$E_2(\boldsymbol{\zeta}) := \frac{1}{\mu} \int_{\Omega} \boldsymbol{\sigma}_h^{\mathbf{d}} : (\boldsymbol{\zeta} - \Pi_h^k(\boldsymbol{\zeta})) + \sum_{e \in \mathcal{E}_h(\Gamma_N)} \int_e \boldsymbol{\xi}_h \cdot (\boldsymbol{\zeta} - \Pi_h^k(\boldsymbol{\zeta})) \boldsymbol{\nu}. \quad (4.14)$$

On the other hand, since  $\mathbf{u}_h|_e \in \mathbf{P}_k(e)$  for each edge  $e \in \mathcal{E}_h$  (in particular for each edge  $e \in \mathcal{E}_h(\Gamma_N)$ ), and  $\nabla \mathbf{u}_h|_T \in \mathbb{P}_{k-1}(T)$  for each  $T \in \mathcal{T}_h$ , the identities (3.10) and (3.11) characterizing  $\Pi_h^k$ , yield, respectively,

$$\int_e (\boldsymbol{\zeta} - \Pi_h^k(\boldsymbol{\zeta})) \boldsymbol{\nu} \cdot \mathbf{u}_h = 0 \quad \forall e \in \mathcal{E}_h(\Gamma_N),$$

and

$$\int_T (\boldsymbol{\zeta} - \Pi_h^k(\boldsymbol{\zeta})) : \nabla \mathbf{u}_h = 0 \quad \forall T \in \mathcal{T}_h.$$

Hence, introducing the above expressions into (4.14), we can write  $E_2(\boldsymbol{\zeta})$  as

$$E_2(\boldsymbol{\zeta}) = \sum_{T \in \mathcal{T}_h} \int_T \left( \frac{1}{\mu} \boldsymbol{\sigma}_h^{\mathbf{d}} - \nabla \mathbf{u}_h \right) : (\boldsymbol{\zeta} - \Pi_h^k(\boldsymbol{\zeta})) + \sum_{e \in \mathcal{E}_h(\Gamma_N)} \int_e (\boldsymbol{\xi}_h + \mathbf{u}_h) \cdot (\boldsymbol{\zeta} - \Pi_h^k(\boldsymbol{\zeta})) \boldsymbol{\nu},$$

from which, applying the Cauchy-Schwarz inequality, the approximation properties (3.14) and (3.16) (with  $m = 1$ ), and the fact that  $\|\boldsymbol{\zeta}\|_{1,\Omega} \leq C \|\boldsymbol{\tau}\|_{\mathbf{div};\Omega}$  (cf. (4.7)), we obtain the required estimate.  $\square$

**Lemma 4.5** *There exists  $C > 0$ , independent of  $\mu$  and  $\alpha$ , such that*

$$\begin{aligned} |E_3(\boldsymbol{\chi})| &\leq C \left\{ \sum_{T \in \mathcal{T}_h} \frac{h_T^2}{\mu^2} \|\text{curl}(\boldsymbol{\sigma}_h^{\mathbf{d}})\|_{0,T}^2 + \sum_{e \in \mathcal{E}_h(\Omega)} \frac{h_e}{\mu^2} \|[(\boldsymbol{\sigma}_h^{\mathbf{d}}) \mathbf{s}]\|_{0,e}^2 + \sum_{e \in \mathcal{E}_h(\Gamma_D)} \frac{h_e}{\mu^2} \|(\boldsymbol{\sigma}_h^{\mathbf{d}}) \mathbf{s}\|_{0,e}^2 \right. \\ &\quad \left. + \sum_{e \in \mathcal{E}_h(\Gamma_N)} h_e \left\| \left( \frac{1}{\mu} \boldsymbol{\sigma}_h^{\mathbf{d}} \right) \mathbf{s} + \frac{d\boldsymbol{\xi}_h}{ds} \right\|_{0,e}^2 \right\}^{1/2} \|\boldsymbol{\tau}\|_{\mathbf{div};\Omega}. \end{aligned}$$

**Proof.** We proceed similarly as in the proof of [23, Lemma 6] (see also [25, Lemma 4.3]). Integrating by parts on each  $T \in \mathcal{T}_h$ , using that  $\underline{\mathbf{curl}}(\boldsymbol{\chi} - \boldsymbol{\chi}_h) \boldsymbol{\nu} = \frac{d}{ds}(\boldsymbol{\chi} - \boldsymbol{\chi}_h)$ , and noting that  $\frac{d\boldsymbol{\xi}_h}{ds} \in \mathbf{L}^2(\Gamma_N)$ , we obtain from (4.13) that

$$\begin{aligned}
E_3(\boldsymbol{\chi}) &= \sum_{T \in \mathcal{T}_h} \int_T \frac{1}{\mu} \boldsymbol{\sigma}_h^{\mathbf{d}} : \underline{\mathbf{curl}}(\boldsymbol{\chi} - \boldsymbol{\chi}_h) + \left\langle \frac{d}{ds}(\boldsymbol{\chi} - \boldsymbol{\chi}_h), \boldsymbol{\xi}_h \right\rangle_{\Gamma_N} \\
&= \sum_{T \in \mathcal{T}_h} \frac{1}{\mu} \left\{ \int_T \mathbf{curl}(\boldsymbol{\sigma}_h^{\mathbf{d}}) \cdot (\boldsymbol{\chi} - \boldsymbol{\chi}_h) - \int_{\partial T} (\boldsymbol{\sigma}_h^{\mathbf{d}})_{\mathbf{s}T} \cdot (\boldsymbol{\chi} - \boldsymbol{\chi}_h) \right\} - \int_{\Gamma_N} \frac{d\boldsymbol{\xi}_h}{ds} \cdot (\boldsymbol{\chi} - \boldsymbol{\chi}_h) \\
&= \sum_{T \in \mathcal{T}_h} \frac{1}{\mu} \int_T \mathbf{curl}(\boldsymbol{\sigma}_h^{\mathbf{d}}) \cdot (\boldsymbol{\chi} - \boldsymbol{\chi}_h) - \sum_{e \in \mathcal{E}_h(\Omega)} \frac{1}{\mu} \int_e [(\boldsymbol{\sigma}_h^{\mathbf{d}})_{\mathbf{s}}] \cdot (\boldsymbol{\chi} - \boldsymbol{\chi}_h) \\
&\quad - \sum_{e \in \mathcal{E}_h(\Gamma_D)} \frac{1}{\mu} \int_e (\boldsymbol{\sigma}_h^{\mathbf{d}})_{\mathbf{s}} \cdot (\boldsymbol{\chi} - \boldsymbol{\chi}_h) - \sum_{e \in \mathcal{E}_h(\Gamma_N)} \int_e \left\{ \left( \frac{1}{\mu} \boldsymbol{\sigma}_h^{\mathbf{d}} \right)_{\mathbf{s}} + \frac{d\boldsymbol{\xi}_h}{ds} \right\} \cdot (\boldsymbol{\chi} - \boldsymbol{\chi}_h).
\end{aligned}$$

Next, since  $\boldsymbol{\chi}_h := \mathbf{I}_h(\boldsymbol{\chi})$ , the approximation properties of  $\mathbf{I}_h$  (cf. Lemma 4.2) yield

$$\|\boldsymbol{\chi} - \boldsymbol{\chi}_h\|_{0,T} \leq c_1 h_T \|\boldsymbol{\chi}\|_{1,\Delta(T)} \quad \forall T \in \mathcal{T}_h, \quad (4.15)$$

and

$$\|\boldsymbol{\chi} - \boldsymbol{\chi}_h\|_{0,e} \leq c_2 h_e^{1/2} \|\boldsymbol{\chi}\|_{1,\Delta(e)} \quad \forall e \in \mathcal{E}_h. \quad (4.16)$$

In this way, applying the Cauchy-Schwarz inequality to each term in the above expression for  $E_3(\boldsymbol{\chi})$ , and making use of the estimates (4.15), (4.16) and (4.7), and the fact that the number of triangles in  $\Delta(T)$  and  $\Delta(e)$  are bounded, we conclude the proof.  $\square$

As a consequence of the previous analysis we can establish the following upper bound for  $|E(\boldsymbol{\tau})|$ .

**Lemma 4.6** *There exists  $C > 0$ , such that*

$$\begin{aligned}
|E(\boldsymbol{\tau})| &\leq C \left\{ \sum_{T \in \mathcal{T}_h} \left\{ \|\mathbf{f} - \mathcal{P}_h^k(\mathbf{f})\|_{0,T}^2 + h_T^2 \left\| \frac{1}{\mu} \boldsymbol{\sigma}_h^{\mathbf{d}} - \nabla \mathbf{u}_h \right\|_{0,T}^2 + \frac{h_T^2}{\mu^2} \|\mathbf{curl}(\boldsymbol{\sigma}_h^{\mathbf{d}})\|_{0,T}^2 \right\} \right. \\
&\quad + \sum_{e \in \mathcal{E}_h(\Omega)} \frac{h_e}{\mu^2} \|[(\boldsymbol{\sigma}_h^{\mathbf{d}})_{\mathbf{s}}]\|_{0,e}^2 + \sum_{e \in \mathcal{E}_h(\Gamma_D)} \frac{h_e}{\mu^2} \|(\boldsymbol{\sigma}_h^{\mathbf{d}})_{\mathbf{s}}\|_{0,e}^2 \\
&\quad \left. + \sum_{e \in \mathcal{E}_h(\Gamma_N)} h_e \left\{ \left\| \left( \frac{1}{\mu} \boldsymbol{\sigma}_h^{\mathbf{d}} \right)_{\mathbf{s}} + \frac{d\boldsymbol{\xi}_h}{ds} \right\|_{0,e}^2 + \|\boldsymbol{\xi}_h + \mathbf{u}_h\|_{0,e}^2 \right\} \right\}^{1/2} \|\boldsymbol{\tau}\|_{\mathbf{div};\Omega}.
\end{aligned}$$

**Proof.** It follows straightforwardly from (4.11) and Lemmas 4.3, 4.4, and 4.5.  $\square$

Having established the above bound for  $|E(\boldsymbol{\tau})|$ , we conclude from Lemma 4.1 that

$$\|(\boldsymbol{\sigma} - \boldsymbol{\sigma}_h, \boldsymbol{\xi} - \boldsymbol{\xi}_h)\|_{H \times Q} \leq C \left\{ \sum_{T \in \mathcal{T}_h} \hat{\theta}_T^2 + \|\mathbf{g} - \boldsymbol{\sigma}_h \boldsymbol{\nu}\|_{-1/2,\Gamma_N}^2 \right\}^{1/2}, \quad (4.17)$$

where

$$\begin{aligned} \widehat{\theta}_T^2 := & \|\mathbf{f} - \mathcal{P}_h^k(\mathbf{f})\|_{0,T}^2 + h_T^2 \left\| \frac{1}{\mu} \boldsymbol{\sigma}_h^d - \nabla \mathbf{u}_h \right\|_{0,T}^2 + \frac{h_T^2}{\mu^2} \|\operatorname{curl}(\boldsymbol{\sigma}_h^d)\|_{0,T}^2 + \sum_{e \in \mathcal{E}(T) \cap \mathcal{E}_h(\Omega)} \frac{h_e}{\mu^2} \|[(\boldsymbol{\sigma}_h^d) \mathbf{s}]\|_{0,e}^2 \\ & + \sum_{e \in \mathcal{E}(T) \cap \mathcal{E}_h(\Gamma_D)} \frac{h_e}{\mu^2} \|(\boldsymbol{\sigma}_h^d) \mathbf{s}\|_{0,e}^2 + \sum_{e \in \mathcal{E}(T) \cap \mathcal{E}_h(\Gamma_N)} h_e \left\{ \left\| \left( \frac{1}{\mu} \boldsymbol{\sigma}_h^d \right) \mathbf{s} + \frac{d\boldsymbol{\xi}_h}{ds} \right\|_{0,e}^2 + \|\boldsymbol{\xi}_h + \mathbf{u}_h\|_{0,e}^2 \right\}. \end{aligned}$$

In order to complete the upper bound for  $\|(\boldsymbol{\sigma}, \boldsymbol{\xi}) - (\boldsymbol{\sigma}_h, \boldsymbol{\xi}_h)\|_{H \times Q}$  in terms of local error indicators, we need to estimate the Neumann residual  $\|\mathbf{g} - \boldsymbol{\sigma}_h \boldsymbol{\nu}\|_{-1/2, \Gamma_N}$ . In fact, we have the following result.

**Lemma 4.7** *Assume that the Neumann datum  $\mathbf{g} \in \mathbf{L}^2(\Gamma_N)$ . Then there exists  $C > 0$ , independent of  $h$ , such that*

$$\|\mathbf{g} - \boldsymbol{\sigma}_h \boldsymbol{\nu}\|_{-1/2, \Gamma_N}^2 \leq C \sum_{e \in \mathcal{E}_h(\Gamma_N)} h_e \|\mathbf{g} - \boldsymbol{\sigma}_h \boldsymbol{\nu}\|_{0,e}^2.$$

**Proof.** Because of the definition of the subspace  $H_h$ , it follows that  $\boldsymbol{\sigma}_h \boldsymbol{\nu}|_{\partial T} \in \mathbf{P}_k(\partial T)$  for all  $T \in \mathcal{T}_h$ , whence it is easy to see that  $\mathbf{g} - \boldsymbol{\sigma}_h \boldsymbol{\nu} \in \mathbf{L}^2(\Gamma_N)$ . Then, from the second equation of the discrete scheme (3.5), we obtain that  $\mathbf{g} - \boldsymbol{\sigma}_h \boldsymbol{\nu}$  is  $\mathbf{L}^2(\Gamma_N)$ -orthogonal to  $Q_h$ , which contains the space of continuous piecewise linear functions. In this way, a straightforward application of [12, Theorem 2] yields

$$\|\mathbf{g} - \boldsymbol{\sigma}_h \boldsymbol{\nu}\|_{-1/2, \Gamma_N}^2 \leq \log \{1 + C_h(\Gamma_N)\} \sum_{\tilde{e} \in \Sigma_{2h}} |\tilde{e}| \|\mathbf{g} - \boldsymbol{\sigma}_h \boldsymbol{\nu}\|_{0, \tilde{e}}^2,$$

where  $C_h(\Gamma_N) := \max \left\{ \frac{|\tilde{e}_i|}{|\tilde{e}_j|} : |i - j| = 1, \tilde{e}_i, \tilde{e}_j \in \Sigma_{2h} \right\}$ . Since each edge  $e \in \Sigma_h$  is contained in a segment  $\tilde{e}$  in  $\Sigma_{2h}$ , and both  $\Sigma_h$  and  $\Sigma_{2h}$  are quasi-uniform, we find that

$$\sum_{\tilde{e} \in \Sigma_{2h}} |\tilde{e}| \|\mathbf{g} - \boldsymbol{\sigma}_h \boldsymbol{\nu}\|_{0, \tilde{e}}^2 \leq \sum_{e \in \mathcal{E}_h(\Gamma_N)} h_e \|\mathbf{g} - \boldsymbol{\sigma}_h \boldsymbol{\nu}\|_{0,e}^2,$$

and deduce the existence of  $C > 0$ , independent of  $h$ , such that  $\log \{1 + C_h(\Gamma_N)\} \leq C$ . Consequently, the above inequality becomes

$$\|\mathbf{g} - \boldsymbol{\sigma}_h \boldsymbol{\nu}\|_{-1/2, \Gamma_N}^2 \leq C \sum_{e \in \mathcal{E}_h(\Gamma_N)} h_e \|\mathbf{g} - \boldsymbol{\sigma}_h \boldsymbol{\nu}\|_{0,e}^2,$$

which finishes the proof.  $\square$

It is important to remark here, according to the statement of [12, Theorem 2], that the uniform regularity of the mesh  $\Sigma_{2h}$  insures that the constant  $C$  in Lemma 4.7 is independent of  $h$ , whence the estimate provided there in terms of the computable local quantities  $\|\mathbf{g} - \boldsymbol{\sigma}_h \boldsymbol{\nu}\|_{0,e}$  becomes suitable for the associated adaptive algorithm. Without that assumption, it would not make sense to apply that theorem, and we would have just to keep the expression  $\|\mathbf{g} - \boldsymbol{\sigma}_h \boldsymbol{\nu}\|_{-1/2, \Gamma_N}$  in the a posteriori error estimator, thus rendering a non-local and hence useless quantity for adaptivity.

Then, as a consequence of Lemmas 4.1 and 4.7, together with the estimate (4.17), we conclude that there exists  $C > 0$ , independent of  $h$ , such that

$$\|(\boldsymbol{\sigma}, \boldsymbol{\xi}) - (\boldsymbol{\sigma}_h, \boldsymbol{\xi}_h)\|_{H \times Q} \leq C \boldsymbol{\theta}, \quad (4.18)$$

where  $\boldsymbol{\theta}$  is the global a posteriori error estimator defined by (4.3) and (4.1).

On the other hand, the upper bound for  $\|\mathbf{u} - \mathbf{u}_h\|_{0,\Omega}$  is quite straightforward from the definition of  $\mathbf{u}$  and  $\mathbf{u}_h$ . Indeed, recalling that

$$\mathbf{u} = \frac{1}{\alpha} \{\mathbf{f} + \mathbf{div}(\boldsymbol{\sigma})\} \quad \text{and} \quad \mathbf{u}_h = \frac{1}{\alpha} \left\{ \mathcal{P}_h^k(\mathbf{f}) + \mathbf{div}(\boldsymbol{\sigma}_h) \right\},$$

we easily obtain

$$\|\mathbf{u} - \mathbf{u}_h\|_{0,\Omega} \leq \frac{1}{\alpha} \left\{ \|\mathbf{f} - \mathcal{P}_h^k(\mathbf{f})\|_{0,\Omega} + \|\boldsymbol{\sigma} - \boldsymbol{\sigma}_h\|_{\mathbf{div};\Omega} \right\}. \quad (4.19)$$

Finally, from (4.19) and (4.18) we have that there exists  $C_{\text{rel}} > 0$  such that

$$\|\mathbf{u} - \mathbf{u}_h\|_{0,\Omega} + \|(\boldsymbol{\sigma} - \boldsymbol{\sigma}_h, \boldsymbol{\xi} - \boldsymbol{\xi}_h)\|_{H \times Q} \leq C_{\text{rel}} \boldsymbol{\theta},$$

which proves the reliability of the estimator  $\boldsymbol{\theta}$ .

### 4.3 Efficiency

In this section we prove the efficiency of our a posteriori error estimator  $\boldsymbol{\theta}$  (lower bound in (4.4)). In other words, we derive suitable upper bounds for the eight terms defining the local error indicator  $\boldsymbol{\theta}_T^2$  (cf. (4.1)). We first notice, using the definitions of  $\mathbf{u}$  (cf. (2.5)) and  $\mathbf{u}_h$  (cf. (4.2)), that

$$\|\mathbf{f} - \mathcal{P}_h^k(\mathbf{f})\|_{0,T}^2 \leq 2\alpha^2 \|\mathbf{u} - \mathbf{u}_h\|_{0,T}^2 + 2\|\boldsymbol{\sigma} - \boldsymbol{\sigma}_h\|_{0,T}^2. \quad (4.20)$$

The upper bounds of the remaining seven terms, which depend on the mesh parameters  $h_T$  and  $h_e$ , will be derived next. To this we proceed as in [13] and [14] (see also [20]), and apply results ultimately based on inverse inequalities (see [15]) and the localization technique introduced in [35], which is based on triangle-bubble and edge-bubble functions. To this end, we now introduce further notations and preliminary results. Given  $T \in \mathcal{T}_h$  and  $e \in \mathcal{E}(T)$ , we let  $\psi_T$  and  $\psi_e$  be the usual triangle-bubble and edge-bubble functions, respectively (see [35, eqs. (1.4) and (1.6)]), which satisfy:

- i)  $\psi_T \in P_3(T)$ ,  $\text{supp}(\psi_T) \subseteq T$ ,  $\psi_T = 0$  on  $\partial T$ , and  $0 \leq \psi_T \leq 1$  in  $T$ .
- ii)  $\psi_e|_T \in P_2(T)$ ,  $\text{supp}(\psi_e) \subseteq \omega_e := \cup\{T' \in \mathcal{T}_h : e \in \mathcal{E}(T')\}$ ,  $\psi_e = 0$  on  $\partial T \setminus e$ , and  $0 \leq \psi_T \leq 1$  in  $\omega_e$ .

We also recall from [34] that, given  $k \in \mathbb{N} \cup \{0\}$ , there exists a linear operator  $L : C(e) \rightarrow C(T)$  that satisfies  $L(p) \in P_k(T)$  and  $L(p)|_e = p \quad \forall p \in P_k(e)$ . A corresponding vectorial version of  $L$ , that is the componentwise application of  $L$ , is denoted by  $\mathbf{L}$ . Additional properties of  $\psi_T$ ,  $\psi_e$  and  $L$  are collected in the following lemma.

**Lemma 4.8** *Given  $k \in \mathbb{N} \cup \{0\}$ , there exist positive constants  $c_1, c_2, c_3$ , and  $c_4$ , depending only on  $k$  and the shape regularity of the triangulations (minimum angle condition), such that for each  $T \in \mathcal{T}_h$  and  $e \in \mathcal{E}(T)$ , there hold*

$$\|\psi_T q\|_{0,T}^2 \leq \|q\|_{0,T}^2 \leq c_1 \|\psi_T^{1/2} q\|_{0,T}^2 \quad \forall q \in P_k(T), \quad (4.21)$$

$$\|\psi_e L(p)\|_{0,T}^2 \leq \|p\|_{0,e}^2 \leq c_2 \|\psi_e^{1/2} p\|_{0,e}^2 \quad \forall p \in P_k(e), \quad (4.22)$$

and

$$c_3 h_e \|p\|_{0,e}^2 \leq \|\psi_e^{1/2} L(p)\|_{0,T}^2 \leq c_4 h_e \|p\|_{0,e}^2 \quad \forall p \in P_k(e). \quad (4.23)$$

**Proof.** See [34, Lemma 4.1]. □

The following inverse estimate will also be used.

**Lemma 4.9** *Let  $l, m \in \mathbb{N} \cup \{0\}$  such that  $l \leq m$ . Then, there exists  $c > 0$ , depending only on  $k, l, m$  and the shape regularity of the triangulations, such that for each  $T \in \mathcal{T}_h$  there holds*

$$|q|_{m,T} \leq c h_T^{l-m} |q|_{l,T} \quad \forall q \in P_k(T). \quad (4.24)$$

**Proof.** See [15, Theorem 3.2.6]. □

The following two lemmas are required for the terms involving the curl operator and the tangential jumps across the edges of  $\mathcal{T}_h$ . Their proofs, which make use of Lemmas 4.8 and 4.9, can be found in [6].

**Lemma 4.10** *Let  $\boldsymbol{\rho}_h \in \mathbb{L}^2(\Omega)$  be a piecewise polynomial of degree  $k \geq 0$  on each  $T \in \mathcal{T}_h$ . In addition, let  $\boldsymbol{\rho} \in \mathbb{L}^2(\Omega)$  be such that  $\text{curl}(\boldsymbol{\rho}) = \mathbf{0}$  on each  $T \in \mathcal{T}_h$ . Then, there exists  $c > 0$ , independent of  $h$ , such that*

$$\|\text{curl}(\boldsymbol{\rho}_h)\|_{0,T} \leq c h_T^{-1} \|\boldsymbol{\rho} - \boldsymbol{\rho}_h\|_{0,T} \quad \forall T \in \mathcal{T}_h. \quad (4.25)$$

**Proof.** See [6, Lemma 4.3]. □

**Lemma 4.11** *Let  $\boldsymbol{\rho}_h \in \mathbb{L}^2(\Omega)$  be a piecewise polynomial of degree  $k \geq 0$  on each  $T \in \mathcal{T}_h$ , and let  $\boldsymbol{\rho} \in \mathbb{L}^2(\Omega)$  be such that  $\text{curl}(\boldsymbol{\rho}) = \mathbf{0}$  in  $\Omega$ . Then, there exists  $c > 0$ , independent of  $h$ , such that*

$$\|[\boldsymbol{\rho}_h \mathbf{s}_T]\|_{0,e} \leq c h_e^{-1/2} \|\boldsymbol{\rho} - \boldsymbol{\rho}_h\|_{0,\omega_e} \quad \forall e \in \mathcal{E}_h. \quad (4.26)$$

**Proof.** It is a slight modification of the proof of [6, Lemma 4.4]. We omit the details here. □

We now apply Lemmas 4.10 and 4.11 to bound two other terms defining  $\theta_T^2$ .

**Lemma 4.12** *There exist  $C_1, C_2 > 0$ , independent of  $h$ , such that*

$$\frac{h_T^2}{\mu^2} \|\text{curl}(\boldsymbol{\sigma}_h^{\text{d}})\|_{0,T}^2 \leq C_1 \|\boldsymbol{\sigma} - \boldsymbol{\sigma}_h\|_{0,T}^2 \quad \forall T \in \mathcal{T}_h. \quad (4.27)$$

and

$$\frac{h_e}{\mu^2} \|[(\boldsymbol{\sigma}_h^{\text{d}}) \mathbf{s}_T]\|_{0,e}^2 \leq C_2 \|\boldsymbol{\sigma} - \boldsymbol{\sigma}_h\|_{0,\omega_e}^2 \quad \forall e \in \mathcal{E}_h(\Omega). \quad (4.28)$$

**Proof.** Applying Lemmas 4.10 and 4.11 to  $\boldsymbol{\rho}_h := \boldsymbol{\sigma}_h^{\text{d}}$  and  $\boldsymbol{\rho} := \boldsymbol{\sigma}^{\text{d}} = \mu \nabla \mathbf{u}$ , and then using the continuity of  $\boldsymbol{\tau} \rightarrow \boldsymbol{\tau}^{\text{d}}$ , we obtain (4.25) and (4.26), respectively. □

The following three lemmas apply Lemmas 4.8 and 4.9 to bound other terms defining  $\theta_T^2$ .

**Lemma 4.13** *There exists  $C_3 > 0$ , independent of  $h$ , such that*

$$h_T^2 \left\| \frac{1}{\mu} \boldsymbol{\sigma}_h^{\text{d}} - \nabla \mathbf{u}_h \right\|_{0,T}^2 \leq C_3 \left\{ \|\mathbf{u} - \mathbf{u}_h\|_{0,T}^2 + h_T^2 \|\boldsymbol{\sigma} - \boldsymbol{\sigma}_h\|_{0,T}^2 \right\} \quad \forall T \in \mathcal{T}_h. \quad (4.29)$$

**Proof.** It is similar to the proof of [25, Lemma 4.13], which is a slight modification of the proof of [13, Lemma 6.3] (see also [20, Lemma 5.5]). In fact, given  $T \in \mathcal{T}_h$  we denote  $\gamma_T := \frac{1}{\mu} \boldsymbol{\sigma}_h^d - \nabla \mathbf{u}_h$  in  $T$ . Then, applying the right hand side of (4.21), using that  $\nabla \mathbf{u} = \frac{1}{\mu} \boldsymbol{\sigma}^d$  in  $\Omega$ , and integrating by parts, we find that

$$\begin{aligned} \|\gamma_T\|_{0,T}^2 &\leq c_1 \|\psi_T^{1/2} \gamma_T\|_{0,T}^2 = c_1 \int_T \psi_T \gamma_T : \left( \frac{1}{\mu} \boldsymbol{\sigma}_h^d - \nabla \mathbf{u}_h \right) \\ &= c_1 \int_T \psi_T \gamma_T : \left\{ \nabla(\mathbf{u} - \mathbf{u}_h) + \frac{1}{\mu} (\boldsymbol{\sigma}_h^d - \boldsymbol{\sigma}^d) \right\} \\ &= -c_1 \left\{ \int_T \mathbf{div}(\psi_T \gamma_T) \cdot (\mathbf{u} - \mathbf{u}_h) + \frac{1}{\mu} \int_T \psi_T \gamma_T : (\boldsymbol{\sigma}^d - \boldsymbol{\sigma}_h^d) \right\}. \end{aligned}$$

Then, applying the Cauchy-Schwarz inequality, the inverse estimate (4.24), the left hand side of (4.21), and the continuity of  $\boldsymbol{\tau} \rightarrow \boldsymbol{\tau}^d$ , we get

$$\|\gamma_T\|_{0,T}^2 \leq C \left\{ h_T^{-1} \|\mathbf{u} - \mathbf{u}_h\|_{0,T} + \|\boldsymbol{\sigma} - \boldsymbol{\sigma}_h\|_{0,T} \right\} \|\gamma_T\|_{0,T},$$

which yields

$$\|\gamma_T\|_{0,T} \leq C \left\{ h_T^{-1} \|\mathbf{u} - \mathbf{u}_h\|_{0,T} + \|\boldsymbol{\sigma} - \boldsymbol{\sigma}_h\|_{0,T} \right\}.$$

This inequality implies (4.29) and completes the proof.  $\square$

**Lemma 4.14** *There exists  $C_4 > 0$ , independent of  $h$ , such that for each  $e \in \mathcal{E}_h(\Gamma_D)$  there holds*

$$\frac{h_e}{\mu^2} \|(\boldsymbol{\sigma}_h^d) \mathbf{s}\|_{0,e}^2 \leq C_4 \|\boldsymbol{\sigma} - \boldsymbol{\sigma}_h\|_{0,T_e}^2. \quad (4.30)$$

where  $T_e$  is the triangle of  $\mathcal{T}_h$  having  $e$  as an edge.

**Proof.** We proceed as in the proof of [25, Lemma 4.15]. In fact, given  $e \in \mathcal{E}_h(\Gamma_D)$  we denote  $\gamma_e := (\boldsymbol{\sigma}_h^d) \mathbf{s}$  on  $e$ . Since  $\mathbf{u} = \mathbf{0}$  on  $\Gamma_D$  we observe that  $(\boldsymbol{\sigma}^d) \mathbf{s} = \mu(\nabla \mathbf{u}) \mathbf{s} = \mathbf{0}$  on  $\Gamma_D$ , and hence  $(\boldsymbol{\sigma}_h^d) \mathbf{s} = (\boldsymbol{\sigma}_h^d - \boldsymbol{\sigma}^d) \mathbf{s}$  on  $e$ . Then, applying (4.22) and the extension operator  $\mathbf{L} : \mathbf{C}(e) \rightarrow \mathbf{C}(T)$ , we obtain that

$$\|\gamma_e\|_{0,e}^2 \leq c_2 \|\psi_e^{1/2} \gamma_e\|_{0,e}^2 = c_2 \int_e \psi_e \gamma_e \cdot (\boldsymbol{\sigma}_h^d \mathbf{s}) = c_2 \int_{\partial T_e} \psi_e \mathbf{L}(\gamma_e) \cdot \{(\boldsymbol{\sigma}_h^d - \boldsymbol{\sigma}^d) \mathbf{s}\}.$$

Now, integrating by parts, and using that  $\mathbf{curl}(\boldsymbol{\sigma}^d) = \mathbf{curl}(\mu \nabla \mathbf{u}) = 0$  in  $\Omega$ , we find that

$$\int_{\partial T_e} \psi_e \mathbf{L}(\gamma_e) \cdot \{(\boldsymbol{\sigma}_h^d - \boldsymbol{\sigma}^d) \mathbf{s}\} = - \int_{T_e} \mathbf{curl}(\psi_e \mathbf{L}(\gamma_e)) : (\boldsymbol{\sigma}_h^d - \boldsymbol{\sigma}^d) + \int_{T_e} \psi_e \mathbf{L}(\gamma_e) \cdot \mathbf{curl}(\boldsymbol{\sigma}_h^d).$$

Then, applying the Cauchy-Schwarz inequality, the inverse estimate (4.24), the continuity of  $\boldsymbol{\tau} \rightarrow \boldsymbol{\tau}^d$ , and noting, thanks to the fact that  $0 \leq \psi_e \leq 1$  and the right-hand side of (4.23), that

$$\|\psi_e \mathbf{L}(\gamma_e)\|_{0,T_e} \leq \|\psi_e^{1/2} \mathbf{L}(\gamma_e)\|_{0,T_e} \leq c_4 h_e^{1/2} \|\gamma_e\|_{0,e},$$

we deduce that

$$\|\gamma_e\|_{0,e}^2 \leq C \left\{ h_{T_e}^{-1} \|\boldsymbol{\sigma} - \boldsymbol{\sigma}_h\|_{0,T_e} + \|\mathbf{curl}(\boldsymbol{\sigma}_h^d)\|_{0,T_e} \right\} h_e^{1/2} \|\gamma_e\|_{0,e},$$

which, using that  $h_e \leq h_{T_e}$ , yields

$$\frac{h_e}{\mu^2} \|\gamma_e\|_{0,e}^2 \leq C \left\{ \|\boldsymbol{\sigma} - \boldsymbol{\sigma}_h\|_{0,T_e}^2 + \frac{h_{T_e}^2}{\mu^2} \|\operatorname{curl}(\boldsymbol{\sigma}_h^d)\|_{0,T_e}^2 \right\}.$$

This inequality and (4.27) imply (4.30), which completes the proof.  $\square$

**Lemma 4.15** *There exists  $C_6 > 0$ , independent of  $h$ , such that*

$$\sum_{e \in \mathcal{E}_h(\Gamma_N)} h_e \left\| \left( \frac{1}{\mu} \boldsymbol{\sigma}_h^d \right) \mathbf{s} + \frac{d\boldsymbol{\xi}_h}{ds} \right\|_{0,e}^2 \leq C_6 \left\{ \sum_{e \in \mathcal{E}_h(\Gamma_N)} \|\boldsymbol{\sigma} - \boldsymbol{\sigma}_h\|_{0,T_e}^2 + \|\boldsymbol{\xi} - \boldsymbol{\xi}_h\|_{0;1/2,\Gamma_N}^2 \right\}, \quad (4.31)$$

where, given  $e \in \mathcal{E}_h(\Gamma_N)$ ,  $T_e$  is the triangle of  $\mathcal{T}_h$  having  $e$  as edge.

**Proof.** We adapt the proof of [23, Lemma 20]. In fact, given  $e \in \mathcal{E}_h(\Gamma_N)$  we let  $\gamma_e := \left( \frac{1}{\mu} \boldsymbol{\sigma}_h^d \right) \mathbf{s} + \frac{d\boldsymbol{\xi}_h}{ds}$  on  $e$ . Then, thanks to (4.22) and the extension operator  $\mathbf{L} : \mathbf{C}(e) \rightarrow \mathbf{C}(T)$ , we obtain that

$$\begin{aligned} \|\gamma_e\|_{0,e}^2 &\leq c_2 \|\psi_e^{1/2} \gamma_e\|_{0,e}^2 = c_2 \int_e \psi_e \gamma_e \cdot \left\{ \left( \frac{1}{\mu} \boldsymbol{\sigma}_h^d \right) \mathbf{s} + \frac{d\boldsymbol{\xi}_h}{ds} \right\} \\ &= \frac{c_2}{\mu} \int_{\partial T_e} \psi_e \mathbf{L}(\gamma_e) \cdot (\boldsymbol{\sigma}_h^d) \mathbf{s} + c_2 \int_e \psi_e \gamma_e \cdot \frac{d\boldsymbol{\xi}_h}{ds}. \end{aligned} \quad (4.32)$$

Next, integrating by parts and using that  $\boldsymbol{\sigma}^d = \mu \nabla \mathbf{u}$  in  $\Omega$ , we find that

$$\int_{\partial T_e} \psi_e \mathbf{L}(\gamma_e) \cdot (\boldsymbol{\sigma}_h^d) \mathbf{s} = - \int_{T_e} \underline{\operatorname{curl}}(\psi_e \mathbf{L}(\gamma_e)) : \boldsymbol{\sigma}_h^d + \int_{T_e} \psi_e \mathbf{L}(\gamma_e) \cdot \operatorname{curl}(\boldsymbol{\sigma}_h^d), \quad (4.33)$$

and

$$\begin{aligned} \int_{T_e} \underline{\operatorname{curl}}(\psi_e \mathbf{L}(\gamma_e)) : \boldsymbol{\sigma}_h^d &= \int_{T_e} \underline{\operatorname{curl}}(\psi_e \mathbf{L}(\gamma_e)) : (\boldsymbol{\sigma}_h^d - \boldsymbol{\sigma}^d) + \int_{T_e} \underline{\operatorname{curl}}(\psi_e \mathbf{L}(\gamma_e)) : \mu \nabla \mathbf{u} \\ &= \int_{T_e} \underline{\operatorname{curl}}(\psi_e \mathbf{L}(\gamma_e)) : (\boldsymbol{\sigma}_h^d - \boldsymbol{\sigma}^d) - \mu \left\langle \frac{d\mathbf{u}}{ds}, \psi_e \mathbf{L}(\gamma_e) \right\rangle_{\partial T_e}, \end{aligned} \quad (4.34)$$

where  $\langle \cdot, \cdot \rangle_{\partial T_e}$  denotes the duality pairing between  $\mathbf{H}^{-1/2}(\partial T_e)$  and  $\mathbf{H}^{1/2}(\partial T_e)$ . In this way, replacing (4.34) into (4.33), and then (4.33) into (4.32), and using that  $\mathbf{u} = -\boldsymbol{\xi}$  on  $\Gamma_N$ , we arrive at

$$\begin{aligned} \|\gamma_e\|_{0,e}^2 &\leq C \left\{ - \int_{T_e} \underline{\operatorname{curl}}(\psi_e \mathbf{L}(\gamma_e)) : (\boldsymbol{\sigma}_h^d - \boldsymbol{\sigma}^d) \right. \\ &\quad \left. + \int_{T_e} \psi_e \mathbf{L}(\gamma_e) \cdot \operatorname{curl}(\boldsymbol{\sigma}_h^d) - \left\langle \frac{d}{ds}(\boldsymbol{\xi} - \boldsymbol{\xi}_h), \psi_e \mathbf{L}(\gamma_e) \right\rangle_e \right\}, \end{aligned} \quad (4.35)$$

where  $\langle \cdot, \cdot \rangle_e$  denotes the duality pairing between  $(\mathbf{H}_{00}^{1/2}(e))'$  and  $\mathbf{H}_{00}^{1/2}(e)$ . Here, as usual,  $H_{00}^{1/2}(e)$  stands for the space of traces on  $e$  of those elements in  $H^1(T_e)$  whose traces vanish on  $\partial T_e \setminus e$ .

Now, since  $\psi_e \gamma_e \in \mathbf{H}_{00}^{1/2}(e)$  for each  $e \in \mathcal{E}_h(\Gamma_N)$ , we can write

$$\sum_{e \in \mathcal{E}_h(\Gamma_N)} h_e \left\langle \frac{d}{ds}(\boldsymbol{\xi} - \boldsymbol{\xi}_h), \psi_e \gamma_e \right\rangle_e = \left\langle \frac{d}{ds}(\boldsymbol{\xi} - \boldsymbol{\xi}_h), \boldsymbol{\gamma} \right\rangle_{\Gamma_N},$$

where  $\gamma$  is the piecewise polynomial defined by  $\gamma|_e := h_e \psi_e \gamma_e$  on each  $e \in \mathcal{E}_h(\Gamma_N)$ . Then, applying the boundedness of the tangential derivative  $\frac{d}{ds} : \mathbf{H}_{00}^{1/2}(\Gamma_N) \rightarrow \mathbf{H}_{00}^{-1/2}(\Gamma_N)$ , employing the inverse estimate  $\|\gamma\|_{0;1/2,\Gamma_N} \leq c h^{-1/2} \|\gamma\|_{0,\Gamma_N}$ , and using that  $h_e \leq h$  and  $0 \leq \psi_e \leq 1$ , we deduce from (4.28) that

$$\begin{aligned} \sum_{e \in \mathcal{E}_h(\Gamma_N)} h_e \left\langle \frac{d}{ds}(\boldsymbol{\xi} - \boldsymbol{\xi}_h), \psi_e \gamma_e \right\rangle_e &\leq C h^{-1/2} \|\boldsymbol{\xi} - \boldsymbol{\xi}_h\|_{0;1/2,\Gamma_N} \|\gamma\|_{0,\Gamma_N} \\ &\leq C \|\boldsymbol{\xi} - \boldsymbol{\xi}_h\|_{0;1/2,\Gamma_N} \left\{ \sum_{e \in \mathcal{E}_h(\Gamma_N)} h_e \|\gamma_e\|_{0,e}^2 \right\}^{1/2}. \end{aligned} \quad (4.36)$$

On the other hand, proceeding as in previous proofs, applying Cauchy-Schwarz's inequality, the inverse estimate (4.24), the fact that  $h_e \leq h_T$ , the inequality

$$\|\psi_e \mathbf{L}(\gamma_e)\|_{0,T_e} \leq c h_e^{1/2} \|\gamma_e\|_{0,e},$$

and the upper bound for  $\frac{h_{T_e}^2}{\mu^2} \|\text{curl}(\boldsymbol{\sigma}_h^d)\|_{0,T_e}^2$  (cf. Lemma 4.12), we are able to show that

$$\begin{aligned} \sum_{e \in \mathcal{E}_h(\Gamma_N)} h_e \int_{T_e} \left\{ -\underline{\text{curl}}(\psi_e \mathbf{L}(\gamma_e)) : (\boldsymbol{\sigma}_h^d - \boldsymbol{\sigma}^d) + \psi_e \mathbf{L}(\gamma_e) \cdot \text{curl}(\boldsymbol{\sigma}_h^d) \right\} \\ \leq C \left\{ \sum_{e \in \mathcal{E}_h(\Gamma_N)} \|\boldsymbol{\sigma} - \boldsymbol{\sigma}_h\|_{0,T_e} \right\}^{1/2} \left\{ \sum_{e \in \mathcal{E}_h(\Gamma_N)} h_e \|\gamma_e\|_{0,e}^2 \right\}^{1/2}. \end{aligned} \quad (4.37)$$

Finally, it is easy to see that (4.35), (4.36), and (4.37) lead to (4.31), thus completing the proof.  $\square$

It is important to remark that the estimate provided by Lemma 4.15 is the only nonlocal bound of the present efficiency analysis. However, under an additional regularity assumption on  $\boldsymbol{\xi}$  we are able to prove the following local bound.

**Lemma 4.16** *Assume that  $\boldsymbol{\xi}|_e \in \mathbf{H}^1(e)$  for each  $e \in \mathcal{E}_h(\Gamma_N)$ . Then there exists  $C > 0$ , independent of  $h$ , such that for each  $e \in \mathcal{E}_h(\Gamma_N)$  there holds*

$$h_e \left\| \left( \frac{1}{\mu} \boldsymbol{\sigma}_h^d \right) \mathbf{s} + \frac{d\boldsymbol{\xi}_h}{ds} \right\|_{0,e}^2 \leq C \left\{ \|\boldsymbol{\sigma} - \boldsymbol{\sigma}_h\|_{0,T_e}^2 + h_e \left\| \frac{d}{ds}(\boldsymbol{\xi} - \boldsymbol{\xi}_h) \right\|_{0,e}^2 \right\},$$

where  $T_e$  is the triangle of  $\mathcal{T}_h$  having  $e$  as an edge.

**Proof.** We adapt the proof of [23, Lemma 21]. To this end, it suffices to reconsider the local estimate (4.35), and observe that, as a consequence of the Cauchy-Schwarz inequality, the last term of it is bounded by  $\left\| \frac{d}{ds}(\boldsymbol{\xi} - \boldsymbol{\xi}_h) \right\|_{0,e} \|\gamma_e\|_{0,e}$ . The rest proceeds exactly as in the last part of the proof of Lemma 4.15. We omit further details.  $\square$

Next, in order to bound the boundary terms given by  $h_e \|\boldsymbol{\xi}_h + \mathbf{u}_h\|_{0,e}^2$ ,  $e \in \mathcal{E}_h(\Gamma_N)$ , we need to recall a discrete trace inequality. In fact, as established by [1, Theorem 3.10] (see also [2, eq. (2.4)]), there exists  $c > 0$ , depending only on the shape regularity of the triangulations, such that for each  $T \in \mathcal{T}_h$  and  $e \in \mathcal{E}(T)$ , there holds

$$\|v\|_{0,e}^2 \leq c \left\{ h_e^{-1} \|v\|_{0,T}^2 + h_e |v|_{1,T}^2 \right\} \quad \forall v \in H^1(T). \quad (4.38)$$

**Lemma 4.17** *There exists  $C_7 > 0$ , independent of  $h$ , such that for each  $e \in \mathcal{E}_h(\Gamma_N)$  there holds*

$$h_e \|\boldsymbol{\xi}_h + \mathbf{u}_h\|_{0,e}^2 \leq C_7 \left\{ h_e \|\boldsymbol{\xi} - \boldsymbol{\xi}_h\|_{0,e}^2 + \|\mathbf{u} - \mathbf{u}_h\|_{0,T_e}^2 + h_{T_e}^2 \|\boldsymbol{\sigma} - \boldsymbol{\sigma}_h\|_{0,T_e}^2 \right\}, \quad (4.39)$$

where  $T_e$  is the triangle having  $e$  as an edge.

**Proof.** We adapt the proof of [23, Lemma 22]. Applying the triangle inequality, the fact that  $\boldsymbol{\xi} = -\mathbf{u}$  on  $\Gamma_N$ , and the discrete trace inequality (4.38), we easily obtain that for each  $e \in \mathcal{E}_h(\Gamma_N)$  there holds

$$\begin{aligned} h_e \|\boldsymbol{\xi}_h + \mathbf{u}_h\|_{0,e}^2 &\leq 2 \left\{ h_e \|\boldsymbol{\xi} - \boldsymbol{\xi}_h\|_{0,e}^2 + h_e \|\mathbf{u}_h - \mathbf{u}\|_{0,e}^2 \right\} \\ &\leq C \left\{ h_e \|\boldsymbol{\xi} - \boldsymbol{\xi}_h\|_{0,e}^2 + \|\mathbf{u} - \mathbf{u}_h\|_{0,T_e}^2 + h_{T_e}^2 |\mathbf{u} - \mathbf{u}_h|_{1,T_e}^2 \right\}. \end{aligned} \quad (4.40)$$

Now, recalling that  $\frac{1}{\mu} \boldsymbol{\sigma}^d = \nabla \mathbf{u}$ , and using the continuity of  $\boldsymbol{\tau} \rightarrow \boldsymbol{\tau}^d$ , we deduce that

$$h_{T_e}^2 |\mathbf{u} - \mathbf{u}_h|_{1,T_e}^2 \leq C \left\{ h_{T_e}^2 \|\boldsymbol{\sigma} - \boldsymbol{\sigma}_h\|_{0,T_e}^2 + h_{T_e}^2 \left\| \frac{1}{\mu} \boldsymbol{\sigma}_h^d - \nabla \mathbf{u}_h \right\|_{0,T_e}^2 \right\}. \quad (4.41)$$

In this way (4.41), (4.40), and the upper bound for  $h_{T_e}^2 \left\| \frac{1}{\mu} \boldsymbol{\sigma}_h^d - \nabla \mathbf{u}_h \right\|_{0,T_e}^2$  (cf. Lemma 4.13) yield (4.39), which finishes the proof.  $\square$

We end the present efficiency analysis with the upper bound for  $h_e \|\mathbf{g} - \boldsymbol{\sigma}_h \boldsymbol{\nu}\|_{0,e}^2$ ,  $e \in \mathcal{E}_h(\Gamma_N)$ .

**Lemma 4.18** *Assume that  $\mathbf{g}$  is piecewise polynomial. Then there exists  $C_8 > 0$ , independent of  $h$ , such that for each  $e \in \mathcal{E}_h(\Gamma_N)$  there holds*

$$h_e \|\mathbf{g} - \boldsymbol{\sigma}_h \boldsymbol{\nu}\|_{0,e}^2 \leq C_8 \left\{ \|\boldsymbol{\sigma} - \boldsymbol{\sigma}_h\|_{0,T_e}^2 + h_{T_e}^2 \|\mathbf{div}(\boldsymbol{\sigma} - \boldsymbol{\sigma}_h)\|_{0,T_e}^2 \right\}, \quad (4.42)$$

where  $T_e$  is the triangle having  $e$  as an edge.

**Proof.** We adapt the proof of [23, Lemma 18]. In fact, given  $e \in \mathcal{E}_h(\Gamma_N)$ , we let  $\boldsymbol{\gamma}_e := \mathbf{g} - \boldsymbol{\sigma}_h \boldsymbol{\nu}$  on  $e$ . Then, employing (4.22), the fact that  $\mathbf{g} = \boldsymbol{\sigma} \boldsymbol{\nu}$  on  $\Gamma_N$ , and the extension operator  $\mathbf{L} : \mathbf{C}(e) \rightarrow \mathbf{C}(T)$ , and then integrating by parts in  $T_e$ , we deduce that

$$\begin{aligned} \|\boldsymbol{\gamma}_e\|_{0,e}^2 &\leq c_2 \|\psi_e^{1/2} \boldsymbol{\gamma}_e\|_{0,e}^2 = c_2 \int_e \psi_e \boldsymbol{\gamma}_e \cdot (\boldsymbol{\sigma} - \boldsymbol{\sigma}_h) \boldsymbol{\nu} = c_2 \int_{\partial T_e} \psi_e \mathbf{L}(\boldsymbol{\gamma}_e) \cdot (\boldsymbol{\sigma} - \boldsymbol{\sigma}_h) \boldsymbol{\nu} \\ &= c_2 \int_{T_e} \left( \nabla(\psi_e \mathbf{L}(\boldsymbol{\gamma}_e)) : (\boldsymbol{\sigma} - \boldsymbol{\sigma}_h) + \psi_e \mathbf{L}(\boldsymbol{\gamma}_e) \cdot \mathbf{div}(\boldsymbol{\sigma} - \boldsymbol{\sigma}_h) \right). \end{aligned}$$

Next, applying Cauchy-Schwarz inequality, the fact that  $0 \leq \psi_e \leq 1$ , and the inverse estimate (4.24), and using from (4.23) that

$$\|\psi_e \mathbf{L}(\boldsymbol{\gamma}_e)\|_{0,T_e} \leq \|\psi_e^{1/2} \mathbf{L}(\boldsymbol{\gamma}_e)\|_{0,T_e} \leq c h_e^{1/2} \|\boldsymbol{\gamma}_e\|_{0,e},$$

we find that

$$\begin{aligned} \|\boldsymbol{\gamma}_e\|_{0,e}^2 &\leq C \left\{ h_{T_e}^{-1} \|\boldsymbol{\sigma} - \boldsymbol{\sigma}_h\|_{0,T_e} + \|\mathbf{div}(\boldsymbol{\sigma} - \boldsymbol{\sigma}_h)\|_{0,T_e} \right\} \|\psi_e \mathbf{L}(\boldsymbol{\gamma}_e)\|_{0,T_e} \\ &\leq C h_e^{1/2} \left\{ h_{T_e}^{-1} \|\boldsymbol{\sigma} - \boldsymbol{\sigma}_h\|_{0,T_e} + \|\mathbf{div}(\boldsymbol{\sigma} - \boldsymbol{\sigma}_h)\|_{0,T_e} \right\} \|\boldsymbol{\gamma}_e\|_{0,e}, \end{aligned}$$

which yields

$$h_e \|\gamma_e\|_{0,e}^2 \leq C \left\{ \|\boldsymbol{\sigma} - \boldsymbol{\sigma}_h\|_{0,T_e}^2 + h_{T_e}^2 \|\mathbf{div}(\boldsymbol{\sigma} - \boldsymbol{\sigma}_h)\|_{0,T_e}^2 \right\}. \quad (4.43)$$

Hence, (4.43) implies (4.42), which completes the proof.  $\square$

If  $\mathbf{g}$  were not piecewise polynomial but sufficiently smooth, then higher order terms given by the errors arising from suitable polynomial approximations would appear in (4.42). This explains the eventual expression *h.o.t.* in (4.4).

Consequently, the efficiency of  $\boldsymbol{\theta}$  follows straightforwardly from the estimate (4.20), together with Lemmas 4.13 throughout 4.18, after summing up over  $T \in \mathcal{T}_h$ .

## 5 Numerical results

In this section, we present some numerical results showing the good performance of the mixed finite element scheme (3.5), confirming the reliability and efficiency of the a posteriori error estimator  $\boldsymbol{\theta}$  derived in Section 4, and showing the behaviour of the associated adaptive algorithm. In all the computations we consider the specific finite element subspaces  $H_h$  and  $Q_h$  given by (3.1) (with  $k = 0$ ) and (3.4), respectively. We begin by introducing additional notations. Indeed, in what follows  $N$  stands for the total number of degrees of freedom (unknowns) of (3.5), which can be proved to behave asymptotically as 3 times the number of elements of each triangulation. Also, the individual and total errors are given by

$$\mathbf{e}(\boldsymbol{\sigma}) := \|\boldsymbol{\sigma} - \boldsymbol{\sigma}_h\|_{\mathbf{div};\Omega}, \quad \mathbf{e}(\boldsymbol{\xi}) := \|\boldsymbol{\xi} - \boldsymbol{\xi}_h\|_{0;1/2,\Gamma_N}, \quad \text{and} \quad \mathbf{e}(\boldsymbol{\sigma}, \boldsymbol{\xi}) := \left\{ [\mathbf{e}(\boldsymbol{\sigma})]^2 + [\mathbf{e}(\boldsymbol{\xi})]^2 \right\}^{1/2},$$

whereas the effectivity index with respect to  $\boldsymbol{\theta}$  is defined by

$$\mathbf{eff}(\boldsymbol{\theta}) := \mathbf{e}(\boldsymbol{\sigma}, \boldsymbol{\xi}) / \boldsymbol{\theta}.$$

Then, we define the experimental rates of convergence

$$\mathbf{r}(\boldsymbol{\sigma}) := \frac{\log(\mathbf{e}(\boldsymbol{\sigma})/\mathbf{e}'(\boldsymbol{\sigma}))}{\log(h/h')}, \quad \mathbf{r}(\boldsymbol{\xi}) := \frac{\log(\mathbf{e}(\boldsymbol{\xi})/\mathbf{e}'(\boldsymbol{\xi}))}{\log(h/h')}, \quad \text{and} \quad \mathbf{r}(\boldsymbol{\sigma}, \boldsymbol{\xi}) := \frac{\log(\mathbf{e}(\boldsymbol{\sigma}, \boldsymbol{\xi})/\mathbf{e}'(\boldsymbol{\sigma}, \boldsymbol{\xi}))}{\log(h/h')},$$

where  $e$  and  $e'$  denote the corresponding errors at two consecutive triangulations with mesh sizes  $h$  and  $h'$ , respectively. Nevertheless, when the adaptive algorithm is applied (see details below), the expression  $\log(h/h')$  appearing in the computation of the above rates is replaced by  $-\frac{1}{2} \log(N/N')$ , where  $N$  and  $N'$  denote the corresponding degrees of freedom of each triangulation. In addition, we also denote by  $\mathbf{e}(p)$ ,  $\mathbf{e}(\mathbf{u})$ ,  $\mathbf{r}(p)$ , and  $\mathbf{r}(\mathbf{u})$  the corresponding errors and experimental rates of convergence for  $p$  and  $\mathbf{u}$  when they are approximated by the postprocessing formulae (3.6) and (4.2).

The examples to be considered in this section are described next. Example 1 is employed to illustrate the performance of the mixed finite element scheme (3.5) and to confirm the reliability and efficiency of the a posteriori error estimator  $\boldsymbol{\theta}$ . Then, Examples 2 and 3 are utilized to show the behaviour of the associated adaptive algorithm, which applies the following procedure from [35]:

- 1) Start with a coarse mesh  $\mathcal{T}_h$ .
- 2) Solve the discrete problem (3.5) for the actual mesh  $\mathcal{T}_h$ .
- 3) Compute  $\theta_T$  (cf. (4.1)) for each triangle  $T \in \mathcal{T}_h$ .

- 4) Evaluate stopping criterion and decide to finish or go to next step.  
5) Use *blue-green* procedure to refine each  $T' \in \mathcal{T}_h$  whose indicator  $\theta_{T'}$  satisfies

$$\theta_{T'} \geq \frac{1}{2} \max \left\{ \theta_T : T \in \mathcal{T}_h \right\}$$

- 6) Define resulting mesh as actual mesh  $\mathcal{T}_h$  and go to step 2.

In Example 1 we consider  $\Omega = ]0, 1]^2$ ,  $\Gamma_D = \{(0, x_2) \in \mathbb{R}^2 : 0 \leq x_2 \leq 1\}$ ,  $\Gamma_N = \Gamma \setminus \bar{\Gamma}_D$ ,  $\mu = 1$ ,  $\alpha = 1$ , and choose the data  $\mathbf{f}$  and  $\mathbf{g}$  so that the exact solution is given for each  $\mathbf{x} := (x_1, x_2)^\mathbf{t} \in \Omega$  by

$$\mathbf{u}(\mathbf{x}) = \begin{pmatrix} \sin^2(4x_1) \cos(4x_2) \sin(4x_2) \\ \sin(4x_1) \cos^2(4x_2) \cos(4x_1) \end{pmatrix}$$

and

$$p(\mathbf{x}) = \cos(4x_1) \cos(4x_2) \exp(-x_1).$$

In Example 2 we consider  $\Omega = ]-1, 1[^2 \setminus ]0, 1]^2$ ,  $\Gamma_D = \{(-1, x_2) \in \mathbb{R}^2 : -1 \leq x_2 \leq 1\}$ ,  $\Gamma_N = \Gamma \setminus \bar{\Gamma}_D$ ,  $\mu = 1$ ,  $\alpha = 1$ , and choose  $\mathbf{f}$  and  $\mathbf{g}$  so that the exact solution is given for each  $\mathbf{x} := (x_1, x_2)^\mathbf{t} \in \Omega$  by

$$\mathbf{u}(\mathbf{x}) = \mathbf{curl} \left( (x_1 + 1)^2 \sqrt{(x_1 - 0.1)^2 + (x_2 - 0.1)^2} \right)$$

and

$$p(\mathbf{x}) = \frac{1}{x_2 + 1.1}.$$

Note that  $\Omega$  is a  $L$ -shaped domain and that  $\mathbf{u}$  and  $p$  are singular at  $(0.1, 0.1)$  and along the line  $x_2 = -1.1$ , respectively. Hence, we should expect regions of high gradients around the origin, which is the middle corner of the  $L$ , and along the line  $x_2 = -1.0$ .

Finally, in Example 3 we consider  $\Omega = ]-1, 1[^2 \setminus ([-1, -0.25] \times [-1, 0.5] \cup [0.25, 1] \times [-1, 0.5])$ ,  $\Gamma_D = \{(x_1, 1) \in \mathbb{R}^2 : -1 \leq x_1 \leq 1\}$ ,  $\Gamma_N = \Gamma \setminus \bar{\Gamma}_D$ ,  $\mu = 1$ ,  $\alpha = 10$ , and choose the data  $\mathbf{f}$  and  $\mathbf{g}$  so that the exact solution is given for each  $\mathbf{x} := (x_1, x_2)^\mathbf{t} \in \Omega$  by

$$\mathbf{u}(\mathbf{x}) = \mathbf{curl} \left( (x_2 - 1)^2 \left\{ \sqrt{(x_1 + 0.3)^2 + (x_2 - 0.45)^2} + \sqrt{(x_1 - 0.3)^2 + (x_2 - 0.45)^2} \right\} \right)$$

and

$$p(\mathbf{x}) = \frac{1}{x_2 + 1.1}.$$

Note that  $\Omega$  is a  $T$ -shaped domain and that  $\mathbf{u}$  and  $p$  are singular at  $(-0.3, 0.45)$  and  $(0.3, 0.45)$ , and along the line  $x_2 = -1.1$ , respectively. Hence, similarly to Example 2, we should expect regions of high gradients around  $(-0.25, 0.5)$  and  $(0.25, 0.5)$ , which are the middle corners of the  $T$ , and along the line  $x_2 = -1.0$ .

In Tables 5.1 and 5.2, we summarize the convergence history of the mixed finite element scheme (3.5) as applied to Example 1, for a sequence of quasi-uniform triangulations of the domain. We notice there that the rate of convergence  $O(h)$  predicted by Theorem 3.2 (when  $s = 1$ ) is attained by all the unknowns, including the postprocessed  $\mathbf{u}$  and  $p$  (cf. Table 5.2). In particular, as observed in the sixth column of Table 5.1, the convergence of  $\boldsymbol{\xi}_h$  is a bit faster than expected, which could correspond to either a superconvergence phenomenon or a special feature of this example. We also remark in this

case the good behaviour of the a posteriori error estimator  $\theta$ . Indeed, we see in Table 5.1 that the effectivity index  $\text{eff}(\theta)$  remains always in a neighborhood of 0.88, which illustrates the reliability and efficiency result provided by Theorem 4.1.

Next, in Tables 5.3, 5.4, 5.5, and 5.6, we provide the convergence history of the uniform and adaptive schemes as applied to Examples 2 and 3. We observe here, as expected, that the errors of the adaptive methods decrease faster than those obtained by the quasi-uniform ones. This fact is better illustrated in Figures 5.1 and 5.3 where we display the total errors  $\mathbf{e}(\boldsymbol{\sigma}, \boldsymbol{\xi})$  vs. the degrees of freedom  $N$  for both refinements. Note that the quasi-uniform curves of these figures consider additional meshes that are not included in Tables 5.3 and 5.5. In addition, the effectivity indexes remain again bounded from above and below, which confirms the reliability and efficiency of  $\theta$  for the associated adaptive algorithm as well. Some intermediate meshes obtained with this procedure are displayed in Figures 5.2 and 5.4. It is important to notice here that the adapted meshes concentrate the refinements around the origin and the line  $x_2 = -1$  in Example 2, and around the points  $(-0.25, 0.5)$  and  $(0.25, 0.5)$  and the line  $x_2 = -1$  in Example 3, which says that the method is in fact able to recognize the regions with high gradients of the solutions. Finally, in order to illustrate the accurateness of the adaptive scheme, in Figures 5.5, 5.6, 5.7, and 5.8, we display some components of the solutions for both examples. The approximate ones are placed at the left side for the field unknowns and identified by red bullets for both components of the boundary unknown  $\boldsymbol{\xi}$ , whereas the exact ones are placed at the right side and identified by continuous lines, respectively. In turn, the components of  $\boldsymbol{\xi}$  are depicted along straight lines beginning at the points  $(-1, -1)$  and  $(-1, 1)$  for the  $L$ -shaped and  $T$ -shaped domains, respectively, and then continuing counterclockwise.

We conclude this paper by emphasizing that we have provided enough support to consider the mixed finite element scheme (3.5) and its associated adaptive algorithm, as valid and competitive alternatives to solve the Brinkman problem in porous media flow.

$N$	$h$	$\mathbf{e}(\boldsymbol{\sigma})$	$\mathbf{r}(\boldsymbol{\sigma})$	$\mathbf{e}(\boldsymbol{\xi})$	$\mathbf{r}(\boldsymbol{\xi})$	$\mathbf{e}(\boldsymbol{\sigma}, \boldsymbol{\xi})$	$\mathbf{r}(\boldsymbol{\sigma}, \boldsymbol{\xi})$	$\text{eff}(\theta)$
1650	1/16	4.183E-00	—	1.744E-01	—	4.186E-00	—	0.8845
2542	1/20	3.353E-00	0.992	1.216E-01	1.607	3.355E-00	0.992	0.8838
3626	1/24	2.798E-00	0.994	9.103E-02	1.581	2.799E-00	0.995	0.8833
4902	1/28	2.400E-00	0.996	7.148E-02	1.564	2.401E-00	0.996	0.8830
6370	1/32	2.101E-00	0.997	5.807E-02	1.553	2.101E-00	0.997	0.8828
8030	1/36	1.868E-00	0.998	4.840E-02	1.545	1.868E-00	0.998	0.8827
14162	1/48	1.402E-00	0.998	3.112E-02	1.533	1.402E-00	0.999	0.8825
25026	1/64	1.051E-00	0.999	2.008E-02	1.521	1.052E-00	0.999	0.8823
55970	1/96	7.011E-01	1.000	1.086E-02	1.513	7.012E-01	1.000	0.8822
99202	1/128	5.259E-01	1.000	7.035E-03	1.509	5.259E-01	1.000	0.8821
154722	1/160	4.207E-01	1.000	5.026E-03	1.507	4.208E-01	1.000	0.8821
302626	1/224	3.005E-01	1.000	3.029E-03	1.505	3.005E-01	1.000	0.8820
616642	1/320	2.104E-01	1.000	1.772E-03	1.503	2.104E-01	1.000	0.8820
887426	1/384	1.753E-01	1.000	1.347E-03	1.503	1.753E-01	1.000	0.8820

Table 5.1: EXAMPLE 1, quasi-uniform scheme

$N$	$h$	$e(\mathbf{u})$	$r(\mathbf{u})$	$e(p)$	$r(p)$
1650	1/16	4.161E-00	—	1.524E-01	—
2542	1/20	3.336E-00	0.991	1.205E-01	1.046
3626	1/24	2.783E-00	0.994	9.978E-02	1.030
4902	1/28	2.388E-00	0.996	8.523E-02	1.021
6370	1/32	2.090E-00	0.997	7.441E-02	1.015
8030	1/36	1.858E-00	0.997	6.604E-02	1.012
14162	1/48	1.395E-00	0.998	4.942E-02	1.007
25026	1/64	1.046E-00	0.999	3.702E-02	1.004
55970	1/96	6.976E-01	1.000	2.466E-02	1.002
99202	1/128	5.233E-01	1.000	1.849E-02	1.001
154722	1/160	4.186E-01	1.000	1.479E-02	1.001
302626	1/224	2.990E-01	1.000	1.056E-02	1.000
616642	1/320	2.093E-01	1.000	7.393E-03	1.000
887426	1/384	1.744E-01	1.000	6.160E-03	1.000

Table 5.2: EXAMPLE 1, quasi-uniform scheme for the postprocessed unknowns

## References

- [1] S. AGMON, Lectures on Elliptic Boundary Value Problems. Van Nostrand, Princeton, New Jersey, 1965.
- [2] D.N. ARNOLD, *An interior penalty finite element method with discontinuous elements*. SIAM Journal on Numerical Analysis, vol. 19, 4, pp. 742-760, (1982).
- [3] D.N. ARNOLD, F. BREZZI AND J. DOUGLAS, *PEERS: A new mixed finite element method for plane elasticity*. Japan Journal of Applied Mathematics, vol. 1, pp. 347-367, (1984).
- [4] D.N. ARNOLD, J. DOUGLAS AND CH.P. GUPTA, *A family of higher order mixed finite element methods for plane elasticity*. Numerische Mathematik, vol. 45, 1, pp. 1-22, (1984).
- [5] I. BABUSKA AND G.N. GATICA, *On the mixed finite element method with Lagrange multipliers*. Numerical Methods for Partial Differential Equations, vol. 19, 2, pp. 192-210, (2003).
- [6] T.P. BARRIOS, G.N. GATICA, M. GONZÁLEZ AND N. HEUER, *A residual based a posteriori error estimator for an augmented mixed finite element method in linear elasticity*. ESAIM: Mathematical Modelling and Numerical Analysis, vol. 40, 5, pp. 843-869, (2006).
- [7] F. BREZZI AND M. FORTIN, *Mixed and Hybrid Finite Element Methods*. Springer Verlag, 1991.
- [8] E. BURMAN AND P. HANSBO, *A unified stabilized method for Stokes' and Darcy's equations*. Journal of Computational and Applied Mathematics, vol. 198, 1, pp. 35-51, (2007).
- [9] Z. CAI, B. LEE AND P. WANG, *Least-squares methods for incompressible Newtonian fluid flow: Linear stationary problems*. SIAM Journal on Numerical Analysis, vol. 42, 2, pp. 843-859, (2004).
- [10] Z. CAI AND G. STARKE, *Least-squares methods for linear elasticity*. SIAM Journal on Numerical Analysis, vol. 42, 2, pp. 826-842, (2004).

$N$	$h$	$e(\sigma)$	$r(\sigma)$	$e(\xi)$	$r(\xi)$	$e(\sigma, \xi)$	$r(\sigma, \xi)$	$\text{eff}(\theta)$
38	1/1	1.319E+01	—	2.048E+01	—	2.435E+01	—	0.4912
306	1/3	1.232E+01	0.154	2.244E-00	0.878	1.252E+01	0.185	0.8055
784	1/5	1.027E+01	0.290	1.374E-00	0.361	1.036E+01	0.291	0.8621
1604	1/7	8.815E-00	0.503	9.752E-01	1.376	8.869E-00	0.516	0.8818
2544	1/9	7.482E-00	0.511	7.269E-01	1.300	7.518E-00	0.519	0.8944
3832	1/11	6.558E-00	0.787	5.625E-01	1.806	6.583E-00	0.796	0.9059
5414	1/13	5.604E-00	0.969	4.515E-01	2.486	5.623E-00	0.981	0.9035
7020	1/15	5.117E-00	0.875	3.803E-01	3.083	5.132E-00	0.889	0.9097
9040	1/17	4.659E-00	0.333	3.337E-01	2.984	4.671E-00	0.349	0.9144
12666	1/20	4.057E-00	0.689	2.906E-01	1.466	4.067E-00	0.693	0.9162
19862	1/25	3.177E-00	1.188	2.117E-01	1.353	3.184E-00	1.188	0.9102
38188	1/35	2.367E-00	0.925	1.212E-01	1.704	2.370E-00	0.928	0.9148
77010	1/50	1.654E-00	1.010	6.695E-02	1.583	1.655E-00	1.011	0.9166
123900	1/63	1.296E-00	1.153	4.562E-02	1.733	1.297E-00	1.154	0.9165
199572	1/80	1.030E-00	0.947	3.141E-02	1.594	1.030E-00	0.947	0.9187
308122	1/100	8.198E-01	1.015	2.235E-02	1.535	8.201E-01	1.016	0.9164
608154	1/140	5.762E-01	1.041	1.328E-02	1.531	5.764E-01	1.041	0.9167
1005626	1/180	4.508E-01	0.980	9.077E-03	1.528	4.509E-01	0.980	0.9170

Table 5.3: EXAMPLE 2, quasi-uniform scheme

- [11] Z. CAI, CH. TONG, P.S. VASSILEVSKI AND CH. WANG, *Mixed finite element methods for incompressible flow: stationary Stokes equations*. Numerical Methods for Partial Differential Equations, vol. 26, 4, pp. 957-978, (2009).
- [12] C. CARSTENSEN, *An a posteriori error estimate for a first-kind integral equation*. Mathematics of Computation, vol 66, 217, pp. 139-155, (1997).
- [13] C. CARSTENSEN, *A posteriori error estimate for the mixed finite element method*. Mathematics of Computation, vol. 66, 218, pp. 465-478, (1997).
- [14] C. CARSTENSEN AND G. DOLZMANN, *A posteriori error estimates for mixed FEM in elasticity*. Numerische Mathematik, vol 81, 2, pp. 187-209, (1998).
- [15] P.G. CIARLET, *The Finite Element Method for Elliptic Problems*. North-Holland, 1978.
- [16] P. CLÉMENT, *Approximation by finite element functions using local regularisation*. RAIRO Modélisation Mathématique et Analyse Numérique, vol. 9, pp. 77-84, (1975).
- [17] V.J. ERVIN, J.S. HOWELL AND I. STANCIULESCU, *A dual-mixed approximation method for a three-field model of a nonlinear generalized Stokes problem*. Computer Methods in Applied Mechanics and Engineering, vol. 197, 33-40, pp. 2886-2900, (2008).
- [18] L. FIGUEROA, G.N. GATICA AND N. HEUER, *A priori and a posteriori error analysis of an augmented mixed finite element method for incompressible fluid flows*. Computer Methods in Applied Mechanics and Engineering, vol. 198, 2, pp. 280-291, (2008).
- [19] L.E. FIGUEROA, L., G.N. GATICA AND A. MÁRQUEZ, *Augmented mixed finite element methods for the stationary Stokes Equations*. SIAM Journal on Scientific Computing, vol. 31, 2, pp. 1082-1119, (2008).

$N$	$h$	$e(\boldsymbol{\sigma})$	$r(\boldsymbol{\sigma})$	$e(\boldsymbol{\xi})$	$r(\boldsymbol{\xi})$	$e(\boldsymbol{\sigma}, \boldsymbol{\xi})$	$r(\boldsymbol{\sigma}, \boldsymbol{\xi})$	$\text{eff}(\boldsymbol{\theta})$
38	1.000	1.319E+01	—	2.048E+01	—	2.435E+01	—	0.4912
98	1.000	1.279E+01	0.065	3.628E−00	3.653	1.329E+01	1.278	0.6523
230	0.707	1.220E+01	0.110	2.454E−00	0.917	1.245E+01	0.154	0.7290
460	0.707	9.830E−00	0.624	1.350E−00	1.724	9.922E−00	0.654	0.7807
932	0.707	6.586E−00	1.134	7.760E−01	1.568	6.632E−00	1.141	0.7521
2218	0.500	4.080E−00	1.105	4.346E−01	1.337	4.103E−00	1.107	0.7408
3656	0.250	3.452E−00	0.669	2.510E−01	2.198	3.461E−00	0.681	0.7793
8136	0.177	2.210E−00	1.115	1.439E−01	1.391	2.214E−00	1.117	0.7579
19186	0.125	1.409E−00	1.050	7.170E−02	1.624	1.410E−00	1.052	0.7256
30258	0.125	1.161E−00	0.848	5.105E−02	1.491	1.162E−00	0.850	0.7619
69016	0.063	7.408E−01	1.090	2.574E−02	1.661	7.412E−01	1.091	0.7299
125774	0.044	5.841E−01	0.792	1.734E−02	1.316	5.844E−01	0.792	0.7594
266526	0.031	3.832E−01	1.123	9.891E−03	1.495	3.833E−01	1.123	0.7307
448650	0.031	3.093E−01	0.823	6.409E−03	1.667	3.093E−01	0.823	0.7593
952510	0.022	2.054E−01	1.087	3.715E−03	1.449	2.055E−01	1.087	0.7352
1603396	0.016	1.637E−01	0.872	2.359E−03	1.743	1.637E−01	0.872	0.7555

Table 5.4: EXAMPLE 2, adaptive scheme

- [20] G.N. GATICA, *A note on the efficiency of residual-based a-posteriori error estimators for some mixed finite element methods*. Electronic Transactions on Numerical Analysis, vol. 17, pp. 218-233, (2004).
- [21] G.N. GATICA, *Analysis of a new augmented mixed finite element method for linear elasticity allowing  $\mathbb{RT}_0 - \mathbb{P}_1 - \mathbb{P}_0$  approximations*. ESAIM Mathematical Modelling and Numerical Analysis, vol. 40, 1, pp. 1-28, (2006).
- [22] GATICA, G.N., GONZÁLEZ, M. AND MEDDAHI, S., *A low-order mixed finite element method for a class of quasi-Newtonian Stokes flows. I: A priori error analysis*. Computer Methods in Applied Mechanics and Engineering, vol. 193, 9-11, pp. 881-892, (2004).
- [23] G.N. GATICA, G. HSIAO, AND S. MEDDAHI, *A residual-based a posteriori error estimator for a two-dimensional fluid-solid interaction problem*. Numerische Mathematik, vol. 114, 1, pp. 63-106, (2009).
- [24] G.N. GATICA, A. MÁRQUEZ AND S. MEDDAHI, *An augmented mixed finite element method for 3D linear elasticity problems*. Journal of Computational and Applied Mathematics, vol. 231, 2, pp. 526-540, (2009).
- [25] G.N. GATICA, A. MÁRQUEZ, AND M. SÁNCHEZ, *Analysis of a velocity-pressure-pseudostress formulation for the stationary Stokes equations*. Computer Methods in Applied Mechanics and Engineering, vol. 199, 17-20, pp. 1064-1079, (2010).
- [26] G.N. GATICA, A. MÁRQUEZ, AND M. SÁNCHEZ, *A priori and a posteriori error analyses of a velocity-pseudostress formulation for a class of quasi-Newtonian Stokes flows*. Computer Methods in Applied Mechanics and Engineering, vol. 200, 17-20, pp. 1619-1636, (2011).

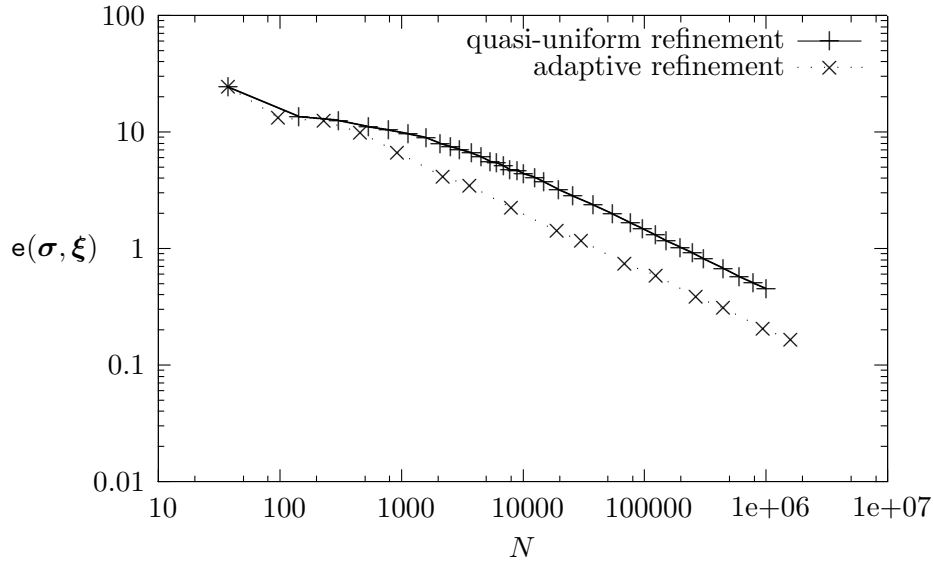


Figure 5.1: EXAMPLE 2,  $e(\sigma, \xi)$  vs.  $N$

- [27] G.N. GATICA, R. OYARZÚA, AND F.J. SAYAS, *Analysis of fully-mixed finite element methods for the Stokes-Darcy coupled problem*. *Mathematics of Computation*, vol. 80, 276, pp. 1911-1948, (2011).
- [28] V. GIRAULT AND P.A. RAVIART, *Finite Element Methods for Navier-Stokes Equations. Theory and Algorithms*. Springer Verlag, 1986.
- [29] P. HANSBO AND M. JUNTUNEN, *Weakly imposed Dirichlet boundary conditions for the Brinkman model of porous media flow*. *Applied Numerical Mathematics*, vol. 59, 6, pp. 1274-1289, (2009).
- [30] R. HIPTMAIR, *Finite elements in computational electromagnetism*. *Acta Numerica*, vol. 11, pp. 237-339, (2002).
- [31] J.S. HOWELL, *Dual-mixed finite element approximation of Stokes and nonlinear Stokes problems using trace-free velocity gradients*. *Journal of Computational and Applied Mathematics*, vol. 231, 2, pp. 780-792, (2009).
- [32] M. JUNTUNEN AND R. STENBERG, *Analysis of finite element methods for the Brinkman problem*. *Calcolo*, vol. 47, 3, pp. 129-147, (2010).
- [33] J.E. ROBERTS AND J.M. THOMAS, *Mixed and Hybrid Methods*. In *Handbook of Numerical Analysis*, edited by P.G. Ciarlet and J.L. Lions, vol. II, Finite Element Methods (Part 1), 1991, Nort-Holland, Amsterdam.
- [34] R. VERFÜRTH, *A posteriori error estimation and adaptive-mesh-refinement techniques*. *Journal of Computational and Applied Mathematics*, vol. 50, 1-3, pp. 67-83, (1994).
- [35] R. VERFÜRTH, *A Review of A Posteriori Error Estimation and Adaptive-Mesh-Refinement Techniques*. Wiley-Teubner (Chichester), 1996.

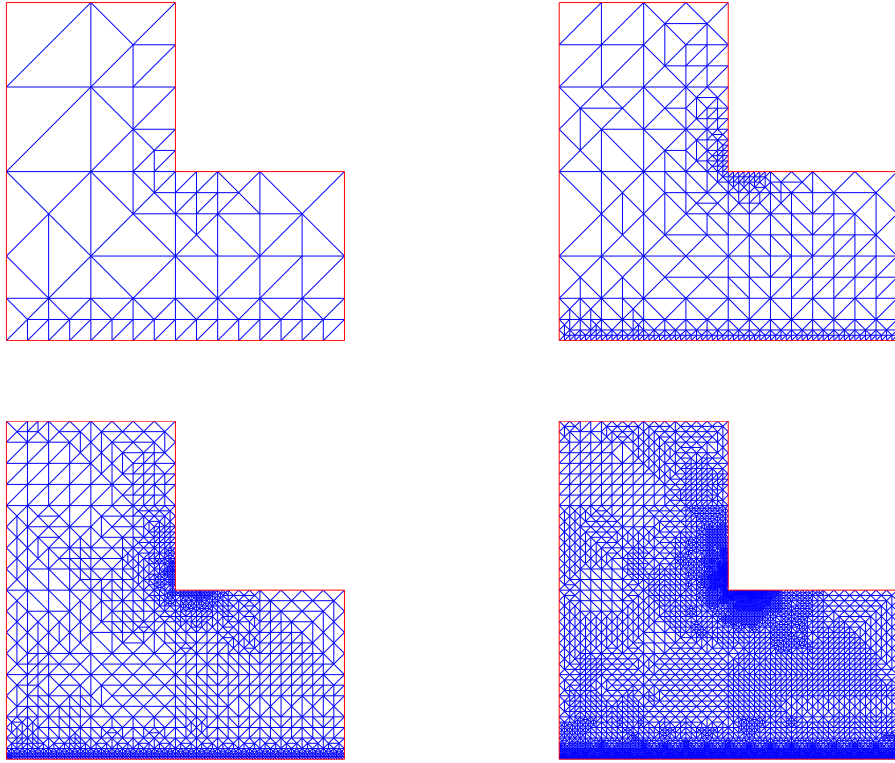


Figure 5.2: EXAMPLE 2, adapted meshes with 460, 2218, 8136, and 30258 degrees of freedom

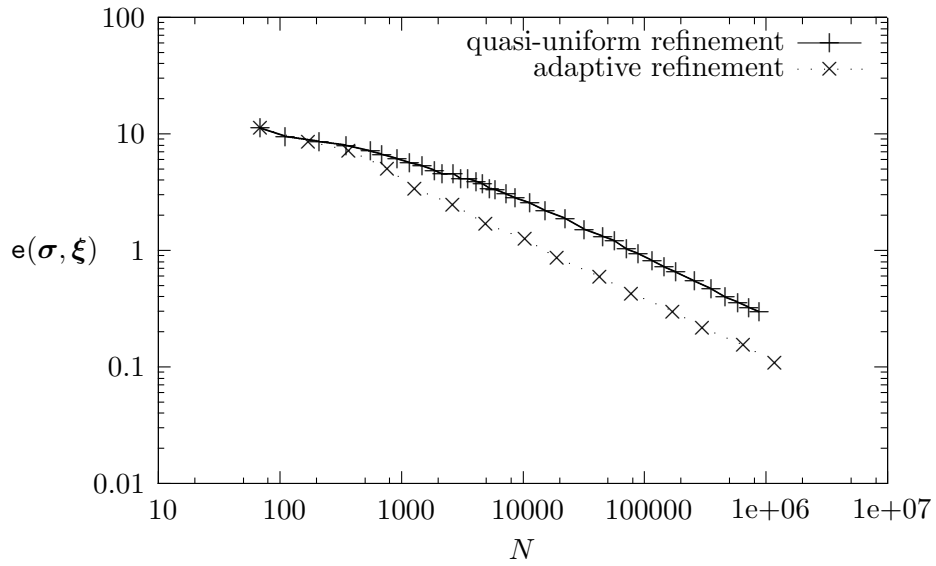


Figure 5.3: EXAMPLE 3,  $e(\sigma, \xi)$  vs.  $N$

$N$	$h$	$e(\sigma)$	$r(\sigma)$	$e(\xi)$	$r(\xi)$	$e(\sigma, \xi)$	$r(\sigma, \xi)$	$\text{eff}(\theta)$
70	1/1	9.848E-00	—	5.408E-00	—	1.124E+01	—	0.4445
212	1/3	8.484E-00	0.151	1.336E-00	2.052	8.588E-00	0.256	0.6332
558	1/5	7.047E-00	0.512	8.293E-01	1.038	7.095E-00	0.520	0.7433
938	1/7	6.096E-00	0.553	5.893E-01	1.194	6.124E-00	0.560	0.7781
1504	1/9	5.309E-00	0.546	4.855E-01	0.877	5.331E-00	0.549	0.8078
2184	1/11	4.475E-00	0.801	3.926E-01	1.597	4.492E-00	0.808	0.8105
3112	1/13	4.086E-00	1.261	3.711E-01	0.948	4.103E-00	1.258	0.8372
4170	1/15	3.888E-00	0.876	3.069E-01	1.176	3.900E-00	0.878	0.8601
5378	1/17	3.409E-00	1.341	2.863E-01	1.112	3.421E-00	1.340	0.8553
7314	1/20	3.035E-00	0.825	2.370E-01	0.702	3.044E-00	0.824	0.8643
11544	1/25	2.555E-00	0.765	1.921E-01	0.722	2.562E-00	0.765	0.8731
22314	1/35	1.882E-00	0.779	1.175E-01	1.585	1.885E-00	0.783	0.8778
45802	1/50	1.314E-00	0.854	7.377E-02	1.426	1.316E-00	0.856	0.8763
72096	1/63	1.022E-00	1.439	5.043E-02	1.683	1.024E-00	1.439	0.8732
116322	1/80	8.207E-01	1.045	3.397E-02	1.699	8.214E-01	1.046	0.8774
182008	1/100	6.501E-01	0.986	2.361E-02	1.632	6.505E-01	0.987	0.8760
357036	1/140	4.700E-01	0.962	1.386E-02	1.514	4.702E-01	0.963	0.8788
588836	1/180	3.602E-01	0.878	9.344E-03	1.498	3.603E-01	0.878	0.8772
880506	1/220	2.959E-01	0.977	6.851E-03	1.513	2.960E-01	0.978	0.8782

Table 5.5: EXAMPLE 3, quasi-uniform scheme

$N$	$h$	$e(\sigma)$	$r(\sigma)$	$e(\xi)$	$r(\xi)$	$e(\sigma, \xi)$	$r(\sigma, \xi)$	$\text{eff}(\theta)$
70	1.000	9.848E-00	—	5.408E-00	—	1.124E+01	—	0.4445
174	0.750	8.525E-00	0.317	1.330E-00	3.081	8.628E-00	0.580	0.6045
372	0.750	7.065E-00	0.494	1.134E-00	0.420	7.155E-00	0.493	0.6693
768	0.500	4.984E-00	0.962	6.372E-01	1.589	5.025E-00	0.975	0.6757
1300	0.375	3.329E-00	1.534	4.396E-01	1.411	3.358E-00	1.532	0.5911
2638	0.250	2.487E-00	0.824	2.396E-01	1.716	2.499E-00	0.835	0.6444
4954	0.188	1.675E-00	1.254	1.474E-01	1.541	1.682E-00	1.256	0.6039
10490	0.125	1.252E-00	0.777	7.860E-02	1.676	1.254E-00	0.782	0.6508
19024	0.094	8.587E-01	1.266	5.092E-02	1.458	8.602E-01	1.267	0.6039
43290	0.063	5.919E-01	0.905	2.562E-02	1.671	5.925E-01	0.907	0.6330
78288	0.047	4.254E-01	1.115	1.779E-02	1.231	4.258E-01	1.115	0.6030
170994	0.031	3.000E-01	0.894	9.242E-03	1.677	3.002E-01	0.895	0.6364
300062	0.023	2.170E-01	1.152	6.305E-03	1.360	2.171E-01	1.152	0.6029
656274	0.016	1.530E-01	0.893	3.340E-03	1.623	1.531E-01	0.893	0.6339
1178168	0.012	1.097E-01	1.139	2.242E-03	1.363	1.097E-01	1.139	0.6030

Table 5.6: EXAMPLE 3, adaptive scheme

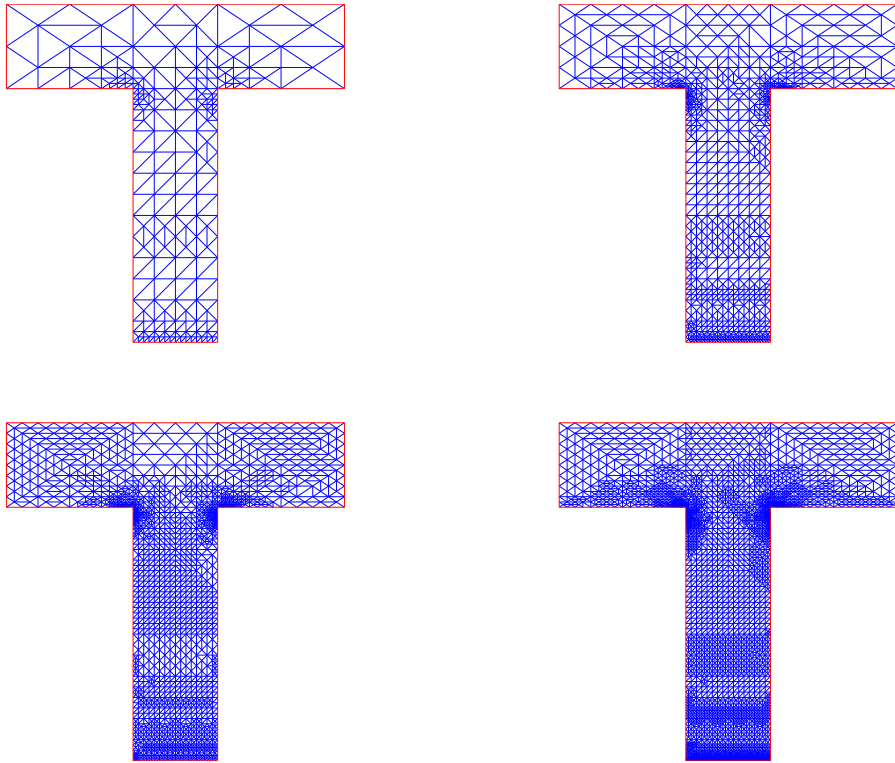


Figure 5.4: EXAMPLE 3, adapted meshes with 1300, 4954, 10490, and 19024 degrees of freedom

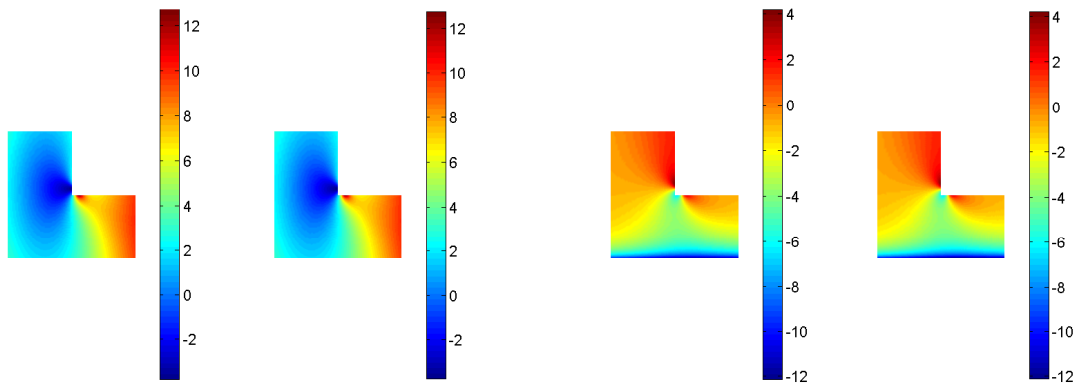


Figure 5.5: EXAMPLE 2, approximate and exact  $\sigma_{21}$  and  $\sigma_{22}$  ( $N = 125774$ ) for adaptive scheme

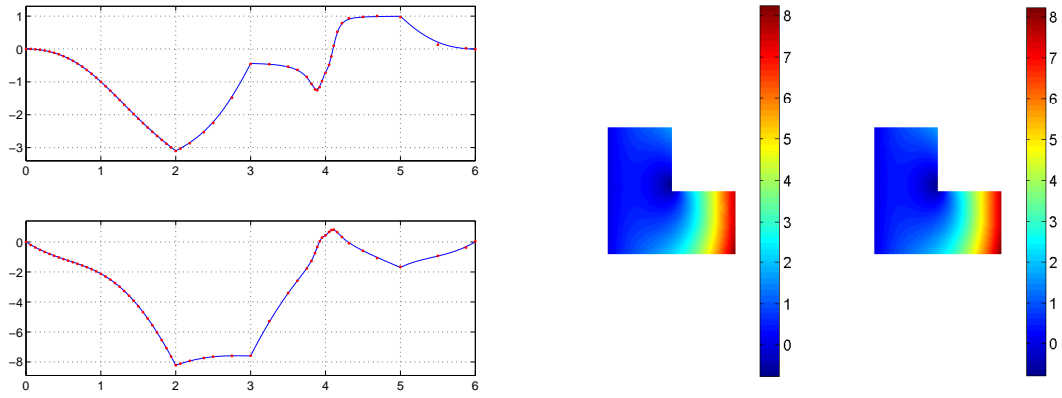


Figure 5.6: EXAMPLE 2, approximate and exact  $\xi$  and  $u_2$  ( $N = 3656, 125774$ ) for adaptive scheme

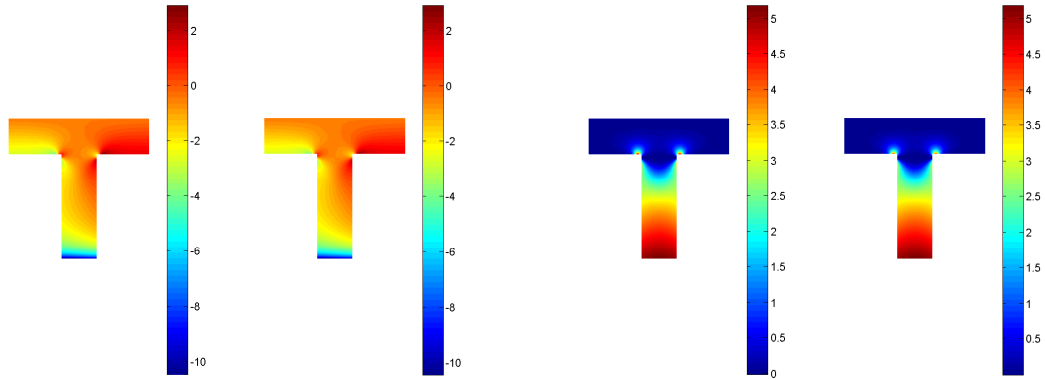


Figure 5.7: EXAMPLE 3, approximate and exact  $\sigma_{11}$  and  $\sigma_{21}$  ( $N = 170994$ ) for adaptive scheme

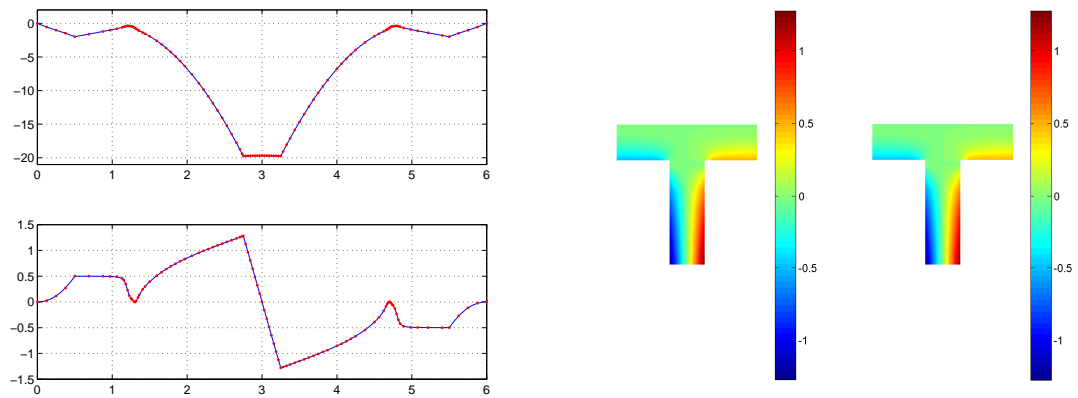


Figure 5.8: EXAMPLE 3, approximate and exact  $\xi$  and  $u_2$  ( $N = 10490, 170994$ ) for adaptive scheme